Degradation of high affinity HuD targets releases Kv1.1 mRNA from miR-129 repression by mTORC1

Natasha M. Sosanya,[1] Peggy P.C. Huang,[1] Luisa P. Cacheaux,[1] Chun Jung Chen,[2] Kathleen Nguyen,[3] Nora I. Perrone-Bizzozero,[4] and Kimberly F. Raab-Graham[1]

[1]Center for Learning and Memory, Section of Neurobiology; and [2]Section of Molecular Genetics and Microbiology; University of Texas at Austin, Austin, TX 78712
[3]College of Medicine, Texas A&M Health Science Center, Bryan, TX 77807
[4]Department of Neurosciences, University of New Mexico Health Sciences Center, Albuquerque, NM 87131

Little is known about how a neuron undergoes site-specific changes in intrinsic excitability during neuronal activity. We provide evidence for a novel mechanism for mTORC1 kinase–dependent translational regulation of the voltage-gated potassium channel Kv1.1 messenger RNA (mRNA). We identified a microRNA, miR-129, that repressed Kv1.1 mRNA translation when mTORC1 was active. When mTORC1 was inactive, we found that the RNA-binding protein, HuD, bound to Kv1.1 mRNA and promoted its translation. Unexpectedly, inhibition of mTORC1 activity did not alter levels of miR-129 and HuD to favor binding to Kv1.1 mRNA. However, reduced mTORC1 signaling caused the degradation of high affinity HuD target mRNAs, freeing HuD to bind Kv1.1 mRNA. Hence, mTORC1 activity regulation of mRNA stability and high affinity HuD-target mRNA degradation mediates the bidirectional expression of dendritic Kv1.1 ion channels.

Introduction

During learning and memory, neurons undergo changes in excitability to enhance their efficacy. One way to modulate neuronal excitability is through regulating the number and composition of ion channels expressed on the cell membrane (Zhang and Linden, 2003; Kim and Hoffman, 2008). Such regulation can be achieved through controlling the local translation of dendritic mRNAs to provide a rapid response to neuronal activity and ensure proper temporal and spatial expression. Our previous work has shown that the local dendritic translation of an ion channel, Kv1.1, mRNA is repressed by mTORC1 kinase activity (Raab-Graham et al., 2006).

Kv1.1 is a dendrotoxin-sensitive voltage-gated potassium channel that is phylogenetically related to the Shaker channel in *Drosophila melanogaster* (Tanouye and Ferrus, 1985; Hopkins et al., 1994). Kv1.1 is characterized as a delayed rectifier potassium channel that controls the frequency of the action potential (Brew et al., 2003). Unlike many ion channels that have redundant functions, Kv1.1 is essential. Mice lacking Kv1.1 either die early or have frequent spontaneous seizures (Smart et al., 1998). Furthermore, haploid insufficiency leads to episodic ataxia, a human neurological disease caused by mutations in Kv1.1 (Zerr et al., 1998). Although a dendrotoxin-sensitive Kv current has been described in CA1 pyramidal dendrites, the molecular identity of this current remains inconclusive (Storm, 1988; Golding et al., 1999; Metz et al., 2007; Chen and Johnston, 2010). Moreover, before our study describing *N*-methyl-D-aspartate receptor (NMDAR)/mTORC1 (mammalian target of rapamycin [mTOR] complex 1)-mediated suppression of Kv1.1 local translation in dendrites, Kv1.1 was considered to be only expressed in axons of hippocampal neurons (Schechter, 1997; Southan and Owen, 1997; Geiger and Jonas, 2000; Monaghan et al., 2001; Raab-Graham et al., 2006; Chen and Johnston, 2010). Here, we report the molecular mechanism for the regulation of dendritic Kv1.1 mRNA translation.

mTOR is a ubiquitous serine/threonine kinase that forms two unique complexes, mTORC1 and mTORC2 (mTOR complex 2). mTORC1 kinase promotes cap-dependent translation via phosphorylation of S6K and 4E-BP, molecules critical for translational initiation. In neurons, mTORC1 kinase is activated by its upstream effectors, including neuronal receptors such as

N.M. Sosanya and P.P.C. Huang contributed equally to this paper.

Correspondence to Kimberly F. Raab-Graham: Kimberly@mail.clm.utexas.edu

Abbreviations used in this paper: aCSF, artificial cerebral spinal fluid; ANOVA, analysis of variance; CR, coding region; dGFP, destabilized GFP; DIV, day in vitro; DTS, dendritic targeting sequence; FL, full length; KD, knockdown; LNA, locked nucleic acid; mTOR, mammalian target of rapamycin; mTRS, mTORC1 kinase repression sequence; NMDAR, *N*-methyl-D-aspartate receptor; qPCR, quantitative PCR; SN, synaptoneurosome; TCEP, tris (2-carboxyethyl) phosphine.

The Rockefeller University Press $30.00
J. Cell Biol. Vol. 202 No. 1 53–69
www.jcb.org/cgi/doi/10.1083/jcb.201212089

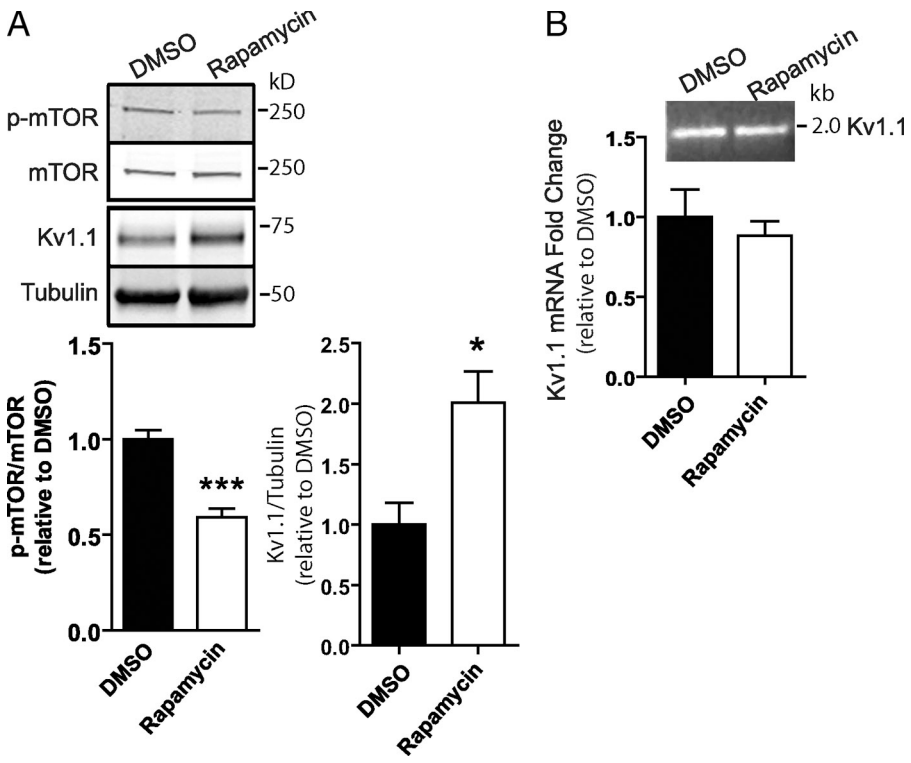

Figure 1. **mTORC1 kinase–dependent repression of Kv1.1 is not a result of mRNA stability.** (A) SNs were isolated from DMSO- or rapamycin-treated DIV 21 cortical neurons. Representative Western blots and quantification indicate the relative level of p-mTOR/mTOR and Kv1.1/tubulin (loading control). ***, $P < 0.001$; *, $P < 0.05$; unpaired Student's *t* test. p-mTOR, $n = 7$; Kv1.1, $n = 5$ over two independent cultures. (B) SN RNA was isolated from DMSO- or rapamycin-treated cortical neurons, and Kv1.1 mRNA was detected via RT-qPCR. Representative DNA gel of RT-qPCR samples showing amplification of a specific Kv1.1 band. DMSO, $n = 5$; rapamycin, $n = 6$ over three independent cultures. Error bars show SEMs.

NMDARs through the signaling molecules phosphoinositide 3-kinase, Akt, and Tsc1/2 (tuberous sclerosis complex proteins 1 and 2; Klann and Dever, 2004; Raab-Graham et al., 2006; Costa-Mattioli et al., 2009). Electrophysiological studies have shown that mTORC1 kinase activity is required for long-term depression and late long-term potentiation (Volk et al., 2007; Ronesi and Huber, 2008; Hoeffer and Klann, 2010). These persistent changes in excitatory neurotransmission have been widely accepted as a model for the cellular basis for learning and memory (Bliss and Lomo, 1973).

Although mTORC1 kinase–dependent translational activation is well studied, how selective mRNAs undergo translational repression when mTORC1 kinase is active remains unclear. Translational repression can be achieved by mRNA-binding molecules such as miRNAs or RNA-binding proteins. miRNAs are ∼18–25-nt-long noncoding RNAs that bind to their target sequences in the 3′ UTR of mRNAs, resulting in reduced protein expression via translational silencing or mRNA degradation (Kosik, 2006; Filipowicz et al., 2008; Bartel, 2009; Konecna et al., 2009).

How mRNA repression is relieved to mediate bidirectional protein expression in an activity-dependent manner is an important question. It was first hypothesized that miRNAs could directly or indirectly affect RNA-binding proteins' ability to interact with their mRNA targets (George and Tenenbaum, 2006). Since then, a growing body of evidence suggests that RNA-binding proteins can displace miRNAs from their target mRNAs even when the binding sites are located many nucleotides apart (Meisner and Filipowicz, 2011; Kundu et al., 2012; Srikantan et al., 2012; Xue et al., 2013).

Here, we report the identification of an miRNA, miR-129, and an RNA-binding protein, HuD, both of which reversibly bind Kv1.1 mRNA when mTORC1 kinase is active and inactive, respectively. Using a local translation assay, we determined that removal of the miR-129 site releases the mTORC1-dependent repression of Kv1.1 mRNA translation. Furthermore, we provide evidence suggesting that HuD high affinity mRNA targets, such as CaMKIIα, GAP-43, and Homer1a, are degraded when mTORC1 is inhibited, allowing HuD to switch targets and overcome miR-129 repression of Kv1.1 mRNA.

Results

mTORC1 kinase activity does not affect Kv1.1 mRNA levels

Previously, we have shown that mTORC1 kinase activity in cortical and hippocampal neurons suppresses the local protein synthesis of Kv1.1 mRNA in neuronal dendrites (Raab-Graham et al., 2006). When mTORC1 kinase activity is inhibited by its specific inhibitor, rapamycin, a significant increase in dendritic Kv1.1 protein is observed (Fig. 1 A; Raab-Graham et al., 2006). To determine the molecular mechanism for the change in Kv1.1 expression in dendrites, we first assessed whether there were corresponding changes in mRNA levels with mTORC1 activity. In cultured neurons (21–28 d in culture), mTORC1 kinase is phosphorylated and thus constitutively active (Fig. 1 A). Synaptoneurosomal preparation was checked for purity by Western blot and immunostaining with a nuclear marker (Fig. S1 A). Treatment with rapamycin inhibits mTORC1 kinase activity by reducing the active p-mTOR over total mTOR ratio to 59.20 ± 4.67% and leads to an approximately twofold increase in Kv1.1 protein (Fig. 1 A, Kv1.1: DMSO [1.00 ± 0.18] and rapamycin [2.00 ± 0.26]; Raab-Graham et al., 2006). We next examined the mRNA levels in synaptoneurosomes (SNs) isolated from

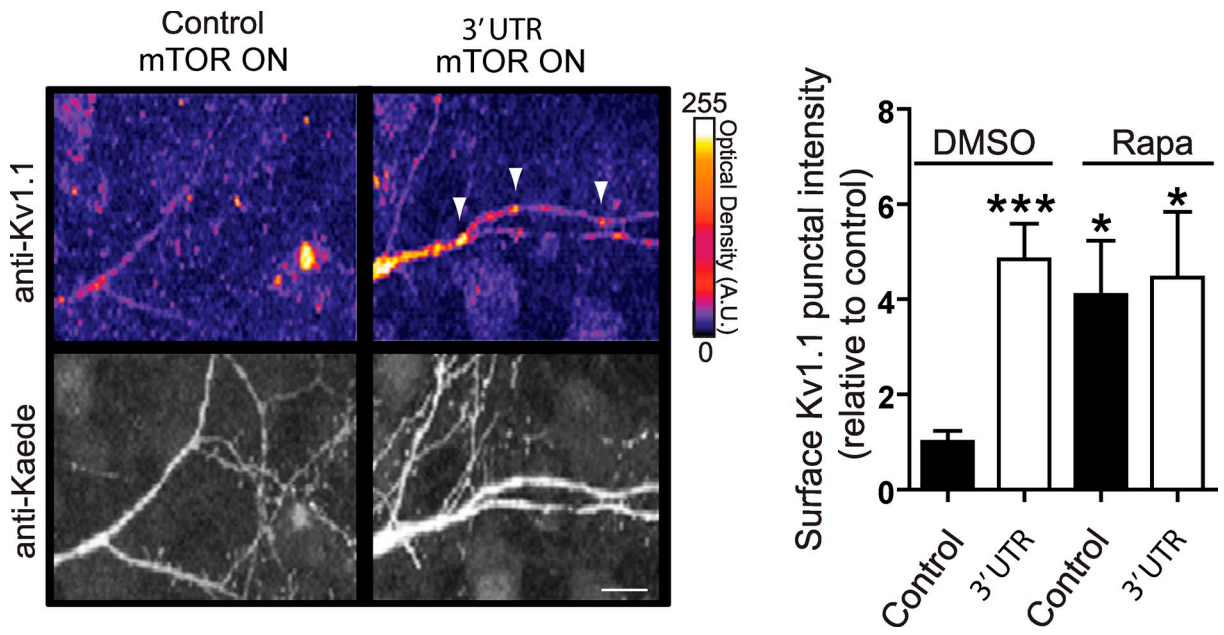

Figure 2. **Overexpression of Kv1.1 3′UTR removes endogenous repression factors, leading to increased Kv1.1 protein.** (left) Representative neurons infected with Sindbis virus coding for control RNA (Kaede-MAP2-DTS) or Kv1.1 3′UTR (DIV 21). Neurons were treated with DMSO or rapamycin. Arrowheads show Kv1.1 puncta (signal). Bar, 20 µm. (right) Quantification of surface expression of Kv1.1. ***, P < 0.001; *, P< 0.05; unpaired Student's *t* test. Control + DMSO: *n* = 16 neurons, 21 dendrites; 3′UTR + DMSO: *n* = 17 neurons, 20 dendrites; control + rapamycin (Rapa): *n* = 7 neurons, 8 dendrites; 3′UTR + rapamycin: *n* = 10 neurons, 11 dendrites. Error bars show SEMs. A.U., arbitrary unit.

cortical neurons treated with rapamycin or carrier (DMSO) by real-time quantitative PCR (qPCR). The representative gel indicates the amplification of a specific Kv1.1 product for each condition (Fig. 1 B, top). Independent of mTORC1 kinase activity, the mRNA level remains constant (Fig. 1 B, bar graph), suggesting a mechanism of altered translation rather than changes in mRNA transport or degradation.

Kv1.1 3′UTR is required for mTORC1 kinase–dependent translational repression

To investigate the molecular mechanism of such translational repression, we first searched for potential regulatory sequences in Kv1.1 mRNA that confer mTORC1 kinase–sensitive repression (Raab-Graham et al., 2006). Previously, we showed local translation of Kv1.1 when mTORC1 kinase is inhibited by blocking NMDARs or by the mTORC1-specific inhibitor rapamycin using the construct containing the coding region (CR) plus the 230-nt 3′UTR of Kv1.1 cloned from synaptoneurosomal cDNA (Raab-Graham et al., 2006). Based on this finding, we hypothesized that a putative mTORC1 kinase repression sequence (mTRS) was present within this 3′UTR.

To verify the importance of the mTRS for Kv1.1 translation in neurons, we designed a competition assay in which excess 3′UTR was introduced to compete for the binding of factors that suppress endogenous Kv1.1, thus resulting in increased Kv1.1 expression (Fig. S1 B). Exogenous 3′UTR containing the putative mTRS was introduced into neurons by a Sindbis virus coding for the fluorescent protein Kaede (Ando et al., 2002) fused to the 3′UTR. To control for nonspecific effects caused by viral infection, neurons were infected with virus coding for Kaede fused to the dendritic targeting sequence (DTS) of MAP2 (Fig. 2; morphological similarity between neurons is demonstrated in Fig. S1 C; Blichenberg et al., 1999). The level of surface Kv1.1 protein was determined by immunocytochemistry on nonpermeabilized neurons using an antibody that recognizes the extracellular domain of Kv1.1 (Tiffany et al., 2000; Raab-Graham et al., 2006). As expected, excess 3′UTR containing the putative mTRS of Kv1.1 mRNA released endogenous Kv1.1 mRNA from repression, resulting in an approximately fivefold (5.41 ± 0.99) increase in Kv1.1 surface protein expression in the dendrites as determined by signal intensity of punctate structures with no significant change in the soma (Fig. 2 and Fig. S1 D). Such an increase is comparable to the levels observed when mTORC1 kinase is inhibited by rapamycin, and excess mTRS does not further increase Kv1.1 expression in rapamycin-treated neurons (Fig. 2). Collectively, these data suggest that the putative mTRS within the 3′UTR is required for repressing Kv1.1 translation in an mTORC1 kinase–sensitive manner.

miR-129 binds Kv1.1 mRNA in an mTORC1 kinase–dependent manner

Notably, sequence alignment of the 3′ UTR containing the mTRS with other mammalian Kv1.1 UTRs revealed a conserved binding site (or seed match sequence) for the miRNA miR-129 (Fig. 3 A). Consistent with Kv1.1 mRNA levels remaining constant with changes in mTOR activity, the complementary of the miR-129 binding site to the 3′UTR sequence is considered to be weak, favoring a role in translational repression over degradation (Filipowicz et al., 2008). To determine whether miR-129 binds to Kv1.1 mRNA and perhaps mediates the mTOR-dependent repression, we used an RNA affinity capture system (Kuwano et al., 2008). RNA was synthesized by in

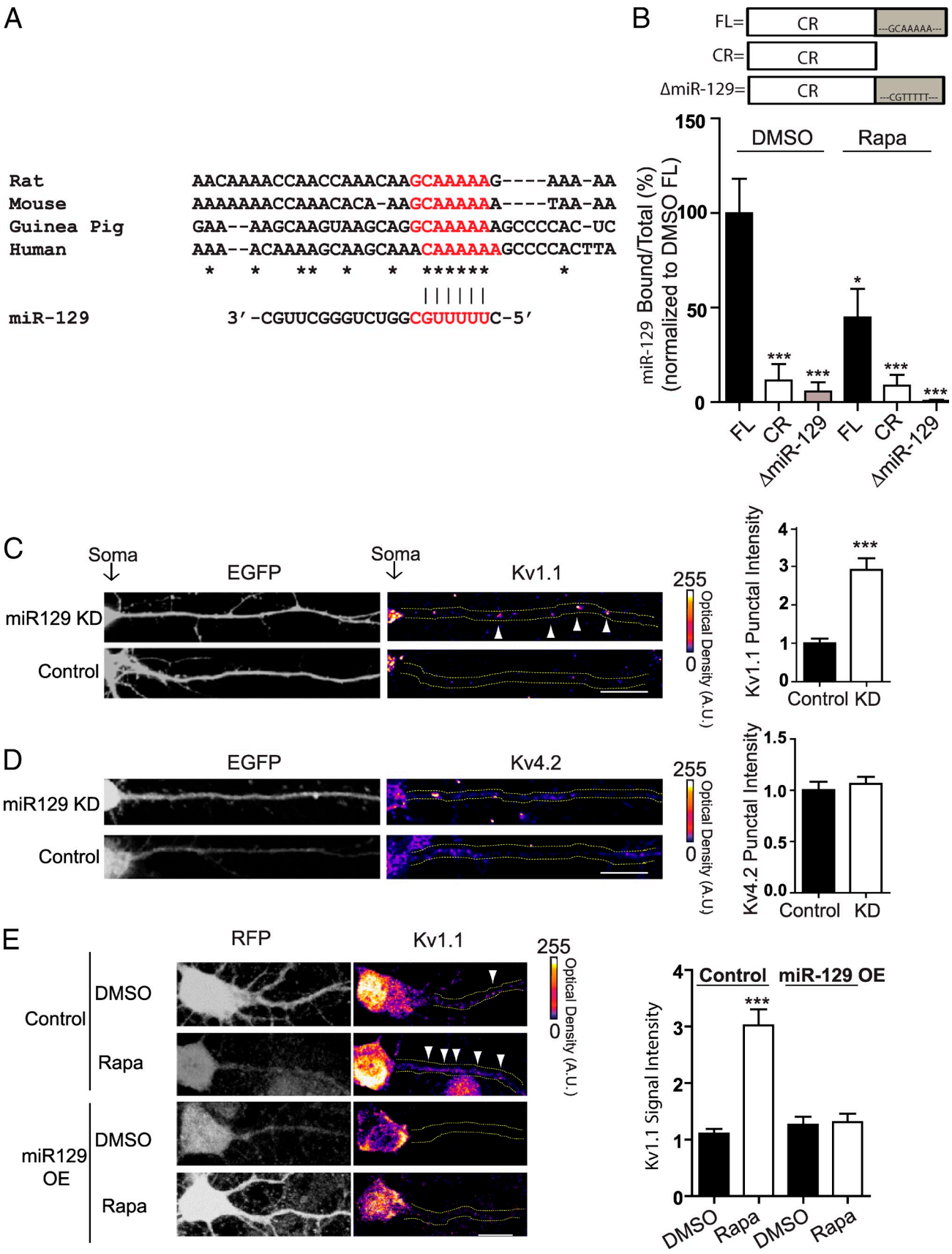

Figure 3. **miR-129 binds Kv1.1 RNA when mTORC1 kinase is active.** (A) Sequence alignment of Kv1.1 3′UTR indicates that the miR-129 seed match sequence (binding to nt 2–8 of miR-129) is conserved among rat, mouse, guinea pig, and human, with nt 1 and 8 being less conserved. The miR-129 binding site is highlighted in red. This motif is considered to be a "weak" binding site, consistent with a role in translational repression over degradation (Vatolin

vitro transcription of cDNAs coding for Kv1.1: full length (FL; CR + 3′UTR), CR, or FL with the predicted miR-129 binding site (seed match sequence) mutated to the complementary sequence (ΔmiR-129; Fig. 3 B, top). The purified RNAs were then labeled with a biotin-linked oligonucleotide (oligo) and served as bait to pull down binding factors from neuronal lysates harvested from cultured cortical neurons treated with DMSO or rapamycin. Factors that bound to Kv1.1 RNA were then precipitated with streptavidin-coated magnetic beads and examined by qPCR for the presence of miR-129 (Fig. S2 A).

When mTORC1 kinase is active and Kv1.1 mRNA translation is suppressed, miR-129 was bound to the FL RNA (Fig. 3 B, bar graph). As a negative control, the RNA affinity capture assay was performed using in vitro synthesized RNA encoding the CR alone or the FL RNA with a mutated miR-129 binding site (ΔmiR-129). As expected, miR-129 binding was significantly reduced under both control conditions relative to the binding of the FL RNA (CR: 11 ± 9%, DMSO; ΔmiR-129: 6 ± 5%, DMSO). However, when mTORC1 kinase was inhibited with rapamycin, miR-129 binding to the FL RNA was reduced to 45 ± 15% (Fig. 3 B). This level was not different from the background binding detected by the two constructs missing the miR-129 seed match sequence. Melt curve analysis was performed to verify that one product was amplified for miR-129 with a signature melting temperature determined by the input (Fig. S2 B). Similar to what we observed in cultured neurons, using solubilized SNs isolated from rat cortices, the FL RNA bound significantly more miR-129 than the CR RNA (52 ± 1% relative to FL; Fig. S2 C). These results suggest that miR-129 binds to the 3′UTR of Kv1.1 mRNA when mTORC1 kinase is active.

miR-129 knockdown (KD) in neurons increases Kv1.1 expression

We next examined the effect of miR-129 on Kv1.1 expression in neurons by transfecting a locked nucleic acid (LNA) probe complementary to miR-129 to knock down its level in neurons. Total Kv1.1 protein was then determined by immunocytochemistry. The protein levels of another dendritic potassium channel, Kv4.2, were determined as a control. The effectiveness of miR-129 KD was established in cortical neurons showing a reduction in miR-129 levels by Northern blot and an increase in the published miR-129 target ERK2 (Fig. S2 D; Wu et al., 2010). If miR-129 suppresses the translation of Kv1.1 in dendrites, knocking down miR-129 will increase the expression of Kv1.1. Indeed, we observed a significant two- to threefold increase in signal intensity of Kv1.1 punctate structures in dendrites when miR-129 was knocked down compared with the negative EGFP or the scrambled LNA controls (Fig. 3 C, miR-129 KD vs. EGFP [2.95 ± 0.3]; and Fig. S2 E, miR-129 KD vs. scrambled LNA [1.9 ± 0.12]). Moreover, there was no change in Kv1.1 intensity in the cell body when miR-129 was knocked down (Fig. S2 E). Furthermore, no significant change was observed in dendritic staining for Kv4.2 (Fig. 3 D and Fig. S2 E). These data suggest that miR-129 suppresses the translation of Kv1.1 mRNA in neuronal dendrites.

Overexpression of miR-129 represses Kv1.1 mRNA translation when mTORC1 kinase is inhibited

To test whether miR-129 mediates repression of Kv1.1 mRNA translation when mTORC1 kinase is active, we transduced neurons with a lentivirus coding for a precursor form of miR-129 (pre–miR-129-2). We predicted that increasing the level of miR-129 would mimic mTORC1 repression of Kv1.1 mRNA translation and thus prevent the increase in dendritic Kv1.1 expression when mTORC1 kinase is inhibited. Indeed, overexpression of miR-129 prevents the observed increase in Kv1.1 dendritic protein with rapamycin, maintaining levels similar to the mTORC1 kinase active state (Fig. 3 E and Fig. S2 F). These data suggest that miR-129 binding to Kv1.1 mRNA is necessary for repressing Kv1.1 translation when mTORC1 is active.

Repression of local protein synthesis of Kv1.1 mRNA in neurons is relieved when the miR-129 binding site is mutated

To further test the functional role of miR-129 in the regulation of Kv1.1 mRNA translation, we performed a local translation assay using Kaede fused to Kv1.1 as a translational reporter (Raab-Graham et al., 2006). Kaede is a fluorescent protein that changes color from green to red upon UV-induced photoconversion (Ando et al., 2002). To assess new protein synthesis, preexistent Kaede-fused protein is first photoconverted to red, and newly synthesized green protein can thus be monitored and quantitated over time. Neurons expressing Kaede-Kv1.1 mRNA

et al., 2006; Grimson et al., 2007). Note that there are an additional 180 nt after the stop codon in the 3′UTR of the rat and mouse sequences that are not present in guinea pig and human sequences. Nucleotide number after the stop codon of each sequence shown: Rat, 181–212 nt; mouse, 177–207 nt; guinea pig, 1–34 nt; human, 1–35 nt. The NCBI accession numbers are rat M26161.1, mouse NM_010595, and human BC101733.1. For guinea pig, the University of California, Santa Cruz genome browser database was used. The sequence is located in scaffold_107:2955798–2955831. The asterisks represent the nucleotides that are conserved between rat, mouse, guinea pig, and human. (B, top) Schematic of RNA fragments used as bait to determine miR-129 binding to Kv1.1. mTRS is indicated by the gray box illustrating the miR-129 seed match sequence (FL) or the mutated sequence (ΔmiR-129). (bottom) qPCR of miR-129 pulled down from DMSO- or rapamycin-treated neurons. *, $P < 0.05$; ***, $P < 0.001$; one-way analysis of variance (ANOVA), Dunnett's posttest compared with the FL DMSO. DMSO: FL $n = 11$, CR $n = 8$, and ΔmiR-129 $n = 5$; rapamycin (Rapa): FL $n = 6$, CR $n = 8$, and ΔmiR-129 $n = 4$ over at least four independent cultures. CR, coding region; FL, full length. (C, left) Representative neurons transfected with EGFP alone (control) or with LNA to specifically knock down miR-129 (KD). Arrowheads indicate Kv1.1 puncta in dendrites. (right) Quantification of dendritic Kv1.1 punctal signal intensity. Number of dendrites: control, $n = 12$; miR-129 KD, $n = 14$. Nine neurons for each condition. ***, $P < 0.001$; unpaired Student's t test. (D, left) Representative neurons transfected with EGFP alone (control) or with LNA against miR-129 (KD). (right) Quantification of dendritic Kv4.2 puncta. Number of dendrites: control, $n = 12$; miR-129 KD, $n = 17$. $n = 8$ and 10 neurons for control and miR-129 KD, respectively. In C and D, yellow dotted lines were drawn to outline representative dendrite in Fig. 3 (C–E). (E, left) Hippocampal neurons transduced with either DsRed control or DsRed pre–miR129-2 lentivirus at DIV 14. DMSO- or rapamycin-treated DIV 21 neurons were stained and imaged for RFP and Kv1.1. (right) Quantification of signal intensity. ***, $P < 0.001$; one-way ANOVA, Tukey posttest. $n = 9$ neurons per treatment. Number of dendrites: DMSO-treated rapamycin control, $n = 17$; $n = 14$ and 15 for miR-129 overexpression (OE). A.U., arbitrary unit. Error bars show SEMs. Bars, 20 µm.

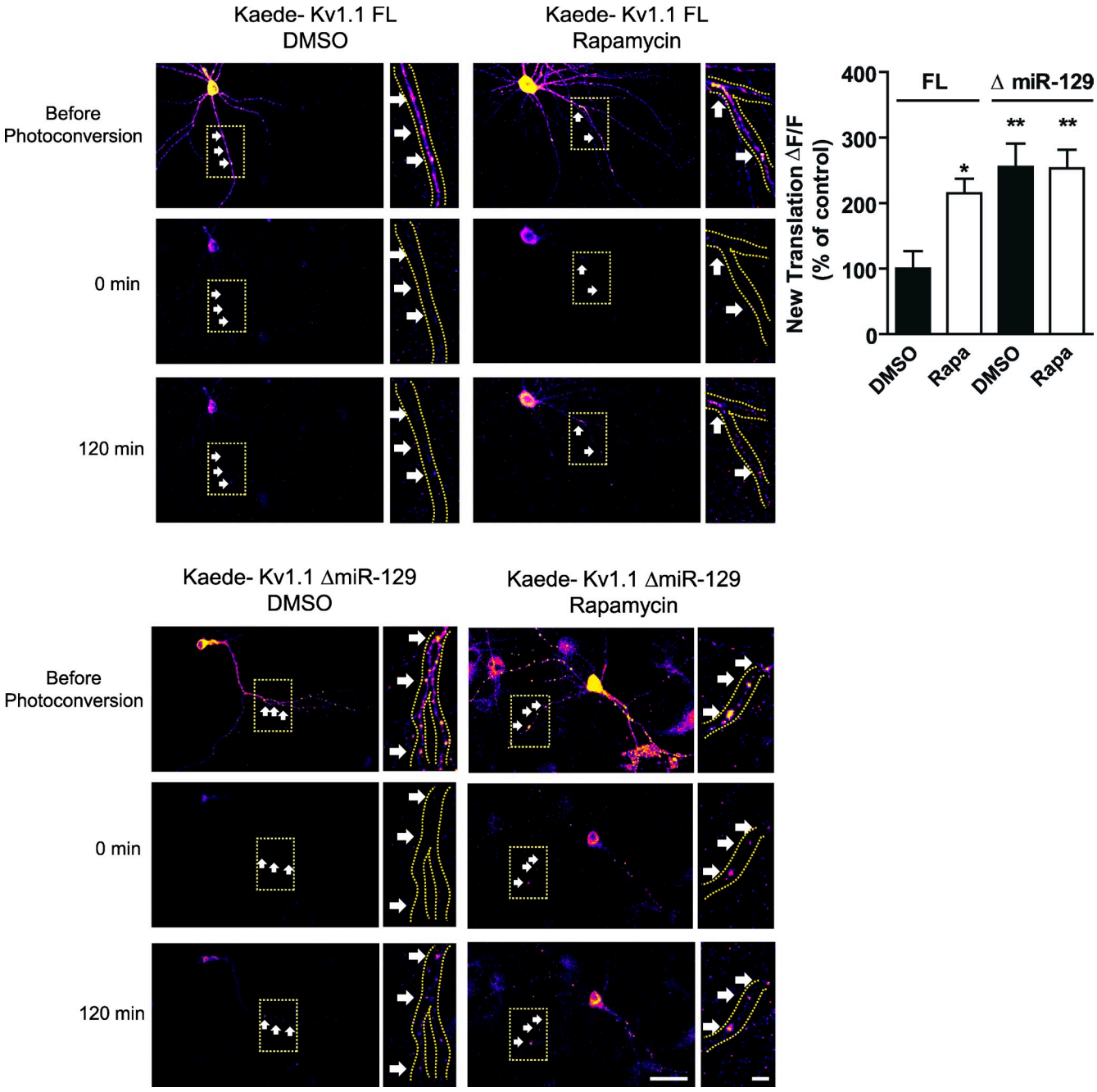

Figure 4. **Mutating the miR-129 seed match sequence in Kaede-Kv1.1 mRNA results in mTORC1-independent new translation in neuronal dendrites.** Live imaging of cultured hippocampal neurons expressing Kaede-Kv1.1 with (top, FL) or without (bottom, ΔmiR-129) seed match sequence of miR-129 in aCSF containing 200 nM DMSO (left, control) or rapamycin (right) before, immediately after (0 time point), and 120 min after UV exposure to photoconvert Kaede-Kv1.1. (left) Entire representative neuron. (right) Enlarged representative dendrite, indicated by arrows, >60 µm from the soma. Bars: (main images) 50 µm; (insets) 10 µm. DMSO: FL, $n = 58$ puncta and ΔmiR129, $n = 67$ puncta; rapamycin (Rapa): FL, $n = 51$ puncta and ΔmiR-129, $n = 64$. *, $P < 0.05$; **, $P < 0.01$; one-way ANOVA, Tukey posttest, relative to Kaede-Kv1.1-FL DMSO. Yellow boxes indicate the region of the dendrite used in the enlarged images. The yellow lines outline the representative dendrite. Error bars show SEMs.

with either intact mTRS or with the predicted miR-129 binding site (seed match) sequence mutated (ΔmiR-129) were imaged for 2 h after complete photoconversion. Detection of new "green" Kaede-Kv1.1 indicates Kv1.1 mRNA translation (Raab-Graham et al., 2006). Previously, we have shown that Kv1.1 protein appears in hot spots within the dendrite when mTORC1 kinase is inhibited. Furthermore, Kv1.1 was found to remain stationary within these hot spots. Transport rates were measured to be <15 µm/h (Raab-Graham et al., 2006). Based on these data, we analyzed only new green Kaede-Kv1.1 puncta >60 µm from the cell body to ensure all new protein was locally synthesized.

Z-stack images detecting the green signal were acquired over time and pseudocolored to reflect the signal intensity of newly synthesized green Kaede-Kv1.1 protein. As shown in Fig. 4, mutating the miR-129 site in the 3′UTR of Kv1.1 mRNA results in an increase in Kv1.1 local mRNA translation by

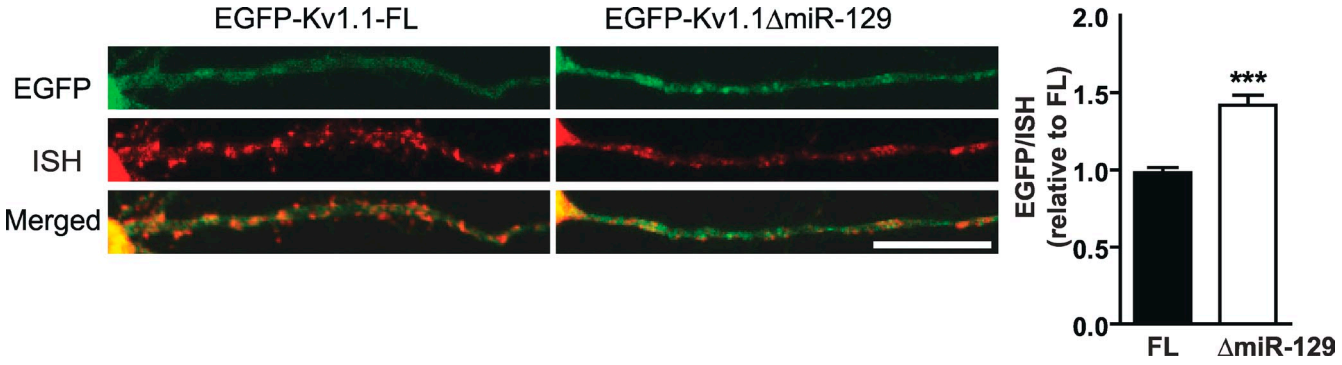

Figure 5. **Mutating the miR-129 seed match sequence in EGFP-Kv1.1 RNA increases protein levels without changing RNA levels.** Representative images of dendritic localization of EGFP-Kv1.1 RNA (red) and protein (green) with the intact (left, FL) or mutated (right, ΔmiR-129) miR-129 binding site revealed by in situ hybridization (ISH) using a digoxigenin-labeled antisense oligo against EGFP. Bar, 20 µM. *n* = 12 and 13 neurons for FL and ΔmiR-129, 40 dendrites each. Error bars show SEMs.

~200% (215.1 ± 22.57%) when mTORC1 kinase was active, similar to the signal observed in neurons expressing Kaede-Kv1.1 with an intact miR-129 site when mTORC1 kinase is inhibited with rapamycin. Furthermore, in the absence of the miR-129 site, rapamycin treatment did not result in further increased translation, suggesting that the miR-129 binding site is the mTRS.

Binding of miR-129 leads to repression rather than degradation of Kv1.1 mRNA in neuronal dendrites

miRNAs have reported roles in both the repression and the degradation of their target mRNAs (Fabian et al., 2010). To verify that miR-129 represses translation without altering mRNA stability, we performed an in situ hybridization using an antisense oligo against EGFP (Wells et al., 2001; Raab-Graham et al., 2006) on neurons expressing EGFP fused to Kv1.1 with either an intact or mutated miR-129 binding site (Fig. 5). If miR-129 binding leads to the degradation of Kv1.1 mRNA, we would predict that more RNA will be detected with the removal of the miR-129 binding site. However, if miR-129 binding represses Kv1.1 mRNA without degradation, removal of the miR-129 site will lead to increased protein expression without altering mRNA levels. As expected, the overall RNA steady-state levels were the same between the two sets of neurons (FL, 1.0 ± 0.06; ΔmiR-129, 1.1 ± 0.06; Fig. S3 A), whereas more protein was detected in the dendrites expressing Kv1.1 with the mutated sequence, as indicated by the ratio of EGFP/in situ hybridization signal (Fig. 5 and Fig. S3 B, FL [1.0 ± 0.06] and ΔmiR-129 [1.4 ± 0.09]). Considering that the Kv1.1 mRNA level remains constant independent of mTORC1 kinase activity (Fig. 1 B) and that mutation of the miR-129 binding site does not change mRNA stability, these data thus support a mechanism of miRNA-mediated repression over degradation.

HuD binds Kv1.1 mRNA when mTORC1 kinase is inactive and overrides mTORC1 kinase–dependent repression

During neuronal transmission, signaling through the NMDAR via the phosphoinositide 3-kinase–mTORC1 pathway represses Kv1.1 mRNA translation. Although such translational repression of Kv1.1 may lead to increased excitability and provide an important positive feedback mechanism for learning and memory, homeostatic mechanisms that lower the membrane potential are required to maintain neuronal stability and allow new learning to occur (Davis and Goodman, 1998; Turrigiano and Nelson, 2000). Because we identified miR-129 as the translational repressor of Kv1.1 mRNA when mTORC1 kinase is active, how inactivating mTORC1 kinase with rapamycin releases such translational repression became the next question.

We first asked whether miR-129 levels would decrease upon rapamycin treatment, thus limiting the amount available to repress translation. To test this possibility, we performed qPCR to detect miR-129 in synaptoneurosomal RNA isolated from neurons in which mTORC1 kinase was active (control with DMSO) or inhibited by rapamycin. Contrary to our prediction, we did not observe a significant change in miR-129 levels between control and rapamycin-treated neurons as determined by both RT-qPCR and Northern blotting (Fig. 6 A).

An alternative possibility is that additional factors interact with Kv1.1 mRNA to relieve repression and promote translation when mTORC1 kinase is inhibited. We therefore searched for RNA-binding proteins that bind Kv1.1 mRNA in an mTORC1 kinase–sensitive manner. To find such candidates, we performed a bioinformatic scan for known binding sites for RNA-binding proteins within the FL Kv1.1 mRNA. We identified three putative HuD binding sites in the CR of Kv1.1 mRNA (Fig. S4 A), consistent with a HuD binding motif previously reported by Wang and Tanaka Hall (2001; x-U/C-U-x-x-U/C-U-U/C; Fig. S4 A). The Hu family of RNA-binding proteins has an established role in stabilizing mRNAs and promoting translation and has been shown to be important for dendritic protein synthesis (Antic et al., 1999; Bolognani and Perrone-Bizzozero, 2008; Tiruchinapalli et al., 2008; Fukao et al., 2009). Moreover, similar to inhibiting mTORC1 kinase with rapamycin to prevent consolidation, mice that overexpress HuD have deficits in learning and memory (Bolognani et al., 2007).

To verify the predicted binding of HuD to Kv1.1 mRNA, coimmunoprecipitation of transfected HEK293T cells was used to assess whether HuD binds directly to Kv1.1 mRNA. HEK293T cells were cotransfected with myc-tagged HuD plus

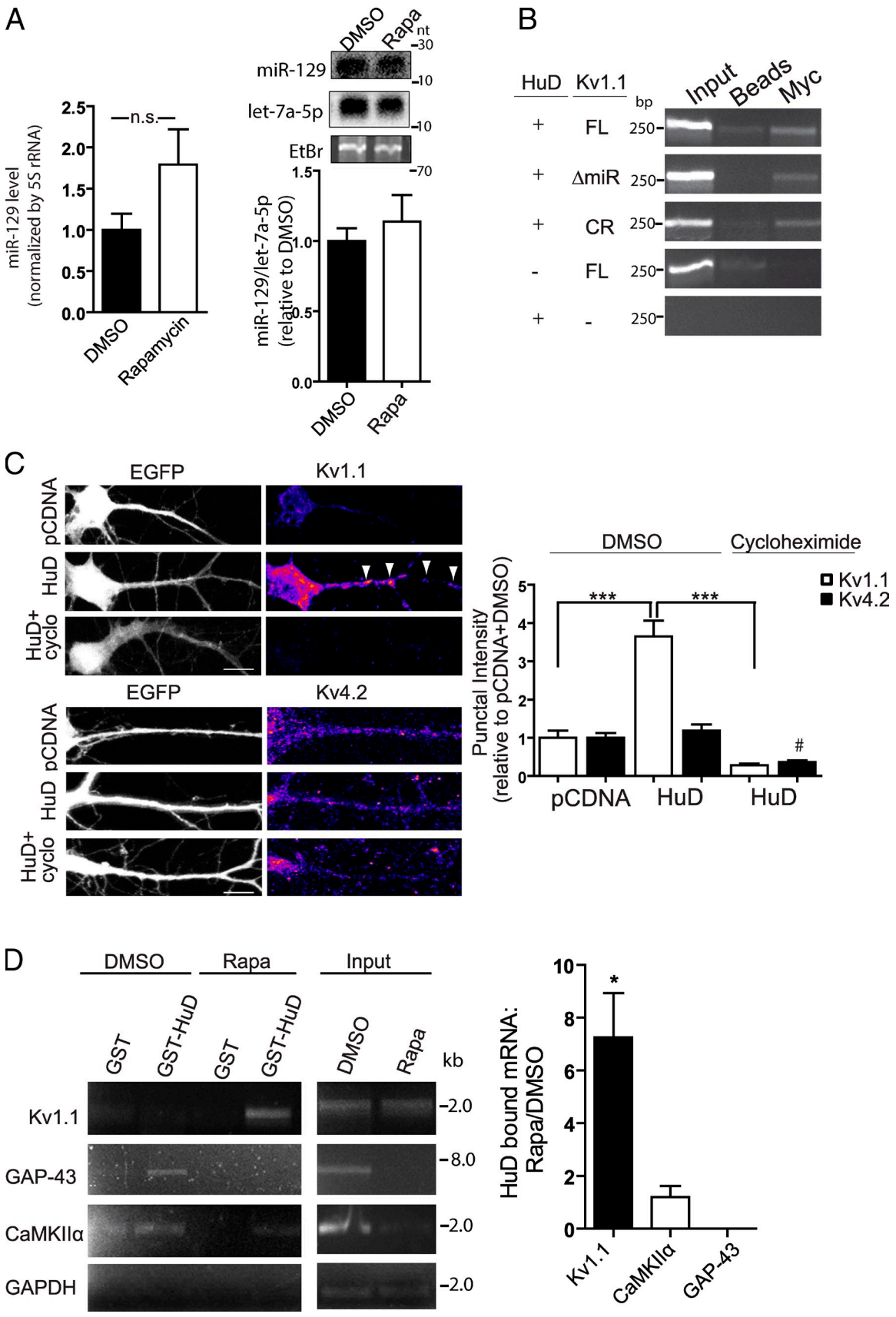

Figure 6. **HuD binds Kv1.1 mRNA when mTORC1 kinase is inhibited and increases Kv1.1 expression that is reversed with cycloheximide.** (A, left) RT-qPCR amplification of miR-129 from neurons treated with DMSO or rapamycin (Rapa). *n* = 3 independent cultures, and each sample was performed in triplicate. (right) Northern blot analysis showed no significant difference in the expression level of miR-129 between neurons treated with DMSO or rapamycin.

either Kaede-Kv1.1 FL, Kaede-Kv1.1 CR, or Kaede-Kv1.1 ΔmiR-129. mRNA protein complexes (messenger RNPs) containing HuD were immunoprecipitated from lysates using a myc-specific antibody. Bound Kv1.1 mRNAs were then detected by RT-PCR using Kv1.1-specific primers. To control for antibody specificity, HEK293T cells were transfected with Kaede-Kv1.1 and an empty vector without myc-HuD. We also included a negative control for nonspecific PCR amplification using myc-HuD and Kaede alone. As expected, Kaede-Kv1.1 FL, CR, and ΔmiR-129 mRNA all copurified with HuD protein (Fig. 6 B). This result is consistent with the predicted HuD binding elements found within the CR of Kv1.1 mRNA (Fig. S4 A). Additionally, Kv1.1-specific PCR products were only detected from RNA immunoprecipitated from lysates expressing HuD and Kv1.1 (Fig. 6 B). Collectively, these results suggest that HuD binds to the CR of Kv1.1 mRNA. A similar mechanism was recently shown for another member of the Hu protein family, HuR, which was found to displace miRNA-induced silencing complexes from target mRNAs even when its binding site and the miRNA site were not adjacent (Kundu et al., 2012).

A direct prediction of this hypothesis is that increasing HuD protein when mTORC1 kinase is active will overcome miR-129–mediated repression of Kv1.1 mRNA. To test this, we overexpressed HuD in cultured hippocampal neurons and measured dendritic Kv1.1 protein. Fig. 6 C shows that under conditions in which mTORC1 kinase is active, neurons overexpressing HuD show a significant three- to fourfold (3.7 ± 0.41) increase of Kv1.1 punctal intensity in dendrites with no significant change in Kv1.1 levels in the cell body (Fig. S4 B). Kv4.2 signal is not affected by HuD overexpression. This increase in Kv1.1 punctal signal is specifically inhibited by the presence of the well-characterized protein synthesis inhibitor cycloheximide (0.3 ± 0.04). Notably, cycloheximide further decreases the levels of both Kv1.1 and Kv4.2 relative to the control condition, indicating a decrease in basal translation (Kv1.1, 0.3 ± 0.04; Kv4.2, 0.4 ± 0.05). These results suggest that overexpression of HuD overrides mTORC1 kinase/miR-129–dependent repression of Kv1.1 mRNA translation.

We next tested whether HuD binding to Kv1.1 mRNA is altered with mTORC1 kinase activity. Purified GST-HuD fusion protein was incubated with total RNA isolated from carrier DMSO- or rapamycin-treated neurons and immunoprecipitated with a pan-Hu antibody (Deschênes-Furry et al., 2007). Bound Kv1.1 mRNAs were then detected by RT-PCR with gene-specific primers. GAP-43 and CaMKIIα mRNAs, known targets of HuD (Bolognani et al., 2006, 2010; Tiruchinapalli et al., 2008), were also assayed in parallel as controls. The differential binding of HuD with different mTORC1 activity to the three mRNAs assayed is reflected by the quantified ratio of mRNA pulled down in rapamycin over DMSO, as shown in Fig. 6 D (note: a ratio of one indicates equal binding under both conditions, a ratio greater than one favors binding in the presence of rapamycin, and a ratio less than one favors binding in DMSO). Interestingly, HuD only binds to GAP-43 mRNA in neurons treated with DMSO (rapamycin/DMSO ratio significantly smaller than 1, one-sample *t* test, $P < 0.05$; Fig. 6 D), whereas HuD binds CaMKIIα mRNA under both conditions (rapamycin/DMSO bound ratio = 1.4 ± 0.4 SD and was not considered significant from 1 by a one-sample *t* test; Fig. 6 D). In contrast, HuD only binds Kv1.1 mRNA in neurons treated with rapamycin (with a ratio of 8.6 ± 0.7 SD, one-sample *t* test, $P < 0.05$; Fig. 6 D). The result that HuD only binds Kv1.1 mRNA in neurons treated with rapamycin supports a role for HuD in promoting Kv1.1 mRNA translation when mTORC1 is inhibited.

HuD binding to Kv1.1 mRNA coincides with the reduced level of other HuD target mRNAs

We next asked whether HuD protein levels increase with mTORC1 kinase inhibition, which could lead to enhanced dendritic Kv1.1 levels. Western blot analysis using a HuD-specific antibody was performed on DMSO- or rapamycin-treated SNs. Contrary to what we expected, HuD levels significantly decrease when mTORC1 was inhibited (Fig. 7 A, DMSO [1.00 ± 0.06] and rapamycin [0.63 ± 0.09]).

We then considered the possible relationship between mTORC1 activity and the abundance of other HuD targets. Notably in Fig. 6 D, the total input of the high affinity HuD-target CaMKIIα with 32 predicted binding sites, some of which overlap (Bolognani et al., 2010), appears to be reduced when mTORC1 kinase is inhibited with rapamycin. To verify this observation in a quantitative manner, we performed RT-qPCR for CaMKIIα and Kv1.1 mRNAs by isolating total RNA from neurons treated with DMSO or rapamycin. As expected, CaMKIIα mRNA was reduced by ∼70% when mTORC1 kinase was inhibited with rapamycin (rapamycin, 33.6 ± 12.5% of control). Furthermore, when we assessed the relative abundance of two

The signal intensity for miR-129 was normalized to the signal intensity for let-7a, which remained constant between DMSO- or rapamycin-treated neurons. As a loading control, ethidium bromide–stained low molecular weight RNA is shown in the bottom blot (labeled as EtBr). n.s., not significant. (B) RT-PCR amplification of Kv1.1 mRNA pulled down by HuD in HEK293T cells. HEK293T cells were cotransfected with myc-HuD and Kaede-Kv1.1 FL, CR, or ΔmiR-129. Antimyc-coated beads were used to pull down HuD bound to Kv1.1 mRNA outlined above. Kv1.1 FL without HuD or Kaede in place of Kv1.1 (bottom) were transfected as controls and show no binding to Kv1.1 mRNA or Kaede RNA alone. *n* = 2 independent cultures. (C, left) Representative neurons (DIV 14) cotransfected with EGFP and either pcDNA or HuD cDNA. Neurons were treated with 50 µM DMSO or cycloheximide, and Kv1.1 and Kv4.2 were detected with specific antibodies. Arrowheads show Kv1.1 puncta (signal). Bars, 20 µm. (right) Quantification of Kv1.1 and Kv4.2 punctal intensity in dendrites. Number of dendrites: DMSO-treated Kv1.1 pCDNA, *n* = 15 and HuD, *n* = 18; Kv4.2 pCDNA, *n* = 17 and HuD, *n* = 16. Cycloheximide (cyclo)-treated Kv1.1 HuD, *n* = 14 and Kv4.2 HuD, *n* = 17. ***, $P < 0.001$; one-way ANOVA, Tukey's posttest. #, Kv4.2 punctal intensity significant from DMSO + HuD. (D) RT-PCR amplification of Kv1.1 (top), GAP-43, or CaMKIIα (middle) mRNA copurified with GST-HuD or GST from DMSO- or rapamycin-treated cortical neurons (DIV 21). (bottom) GAPDH mRNA was detected in input but not pull-down. The ratio (rapamycin/DMSO; right of the images) is determined by subtracting signal intensity of the background GST band from the specific GST-HuD band and normalizing each band by their respective GAPDH input mRNA levels. HuD-RNA pull-down was replicated with three independent cultures for Kv1.1 mRNA and two independent cultures for CaMKIIα and GAP-43 mRNA. Significance for each mRNA was determined by a single Student's *t* test. *, $P < 0.05$, indicating the binding is significantly different from 1. A value of 1 suggests equal binding in both treatments. Error bars show SEMs. rRNA, ribosomal RNA.

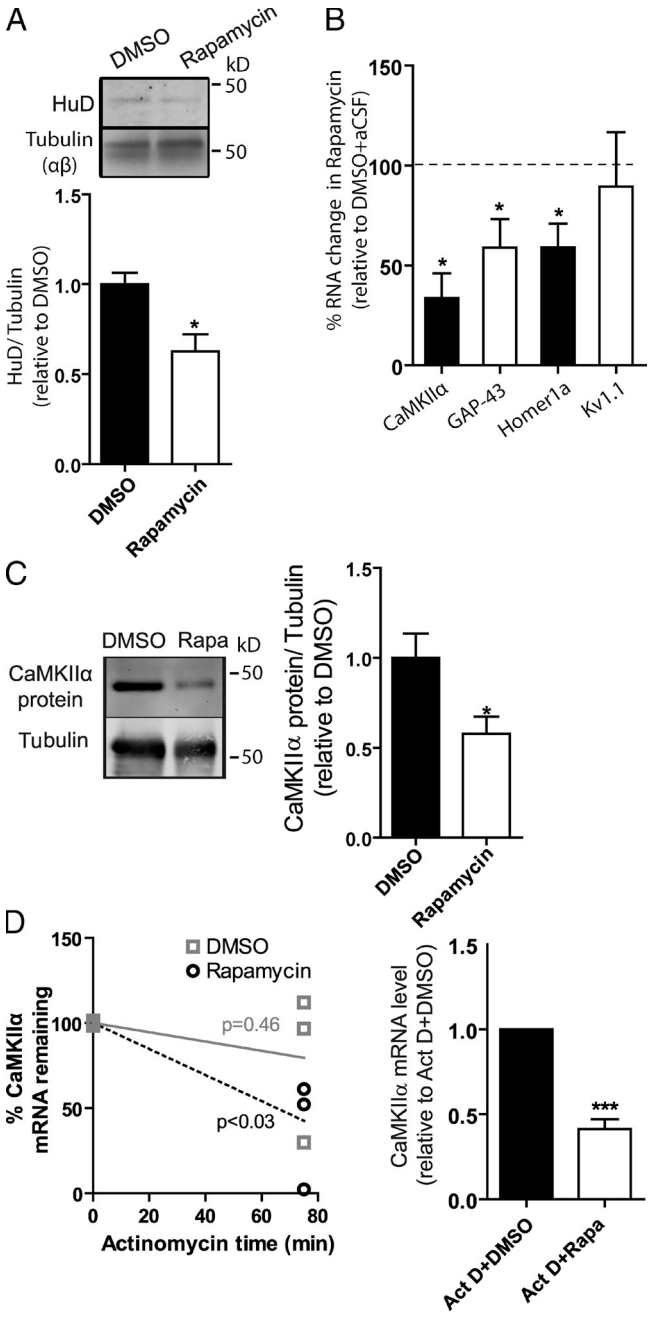

Figure 7. **HuD binding to Kv1.1 mRNA coincides with reduced levels of other HuD-target mRNAs.** (A) Western blot analysis of HuD from SNs isolated from neurons treated with DMSO or rapamycin. DMSO, *n* = 3; rapamycin (Rapa), *n* = 4 over two independent cultures. (B) RT-qPCR analysis of CaMKIIα, GAP-43, Homer1a, and Kv1.1 mRNA isolated from control or 200 nM rapamycin-treated neurons normalized to the internal housekeeping gene, GAPDH, which remains constant between the two conditions. CaMKIIα and Kv1.1, *n* = 3; GAP-43, *n* = 5; Homer1a, *n* = 4; three to five independent cultures. Control was normalized to 100% and is indicated by dotted line on the graph. The mRNA target of HuD is shown as percent remaining after rapamycin treatment. One-sample Student's *t* test was performed to determine statistical significance from control. (C) Representative blot and quantification of SN CaMKIIα protein isolated from DMSO- or rapamycin-treated cortical neurons. DMSO, *n* = 5; rapamycin, *n* = 6. (D) Neurons were treated with 12 µM Actinomycin D (Act D) for 4–5 h before treating with DMSO or rapamycin for 75 min. Degradation was measured by RT-qPCR for CaMKIIα mRNA and reported as the percent decrease with the addition of rapamycin relative to actinomycin alone. *n* = 5 per treatment. The solid line is connecting the mean for actinomycin alone to the mean for 75- min DMSO + actinomycin treatment. The dotted line is connecting the mean for actinomycin alone to the mean for 75-min rapamycin + actinomycin treatment. *, P < 0.05; ***, P < 0.001. Error bars show SEMs.

additional HuD targets, GAP-43 and Homer1a, we found they were both reduced by ∼40% and were significantly different from control (GAP-43: rapamycin, 58.9 ± 14% of control; Homer1a: rapamycin, 59 ± 12% of control; Fig. 7 B). In contrast, Kv1.1 mRNA levels remained the same between the two conditions (Kv1.1: rapamycin, 89 ± 27% of control; Fig. 6 D, input; and Fig. 7 B). Moreover, the reduction of CaMKIIα mRNA is also reflected by the reduced protein level when mTORC1 kinase is inhibited (Fig. 7 C). Collectively, these data led us to consider the possibility that HuD switches its targets in accordance with the mRNAs that are available to be translated.

To determine whether mTORC1 activity affects high affinity HuD-target mRNA levels at the transcriptional level or causes mRNA degradation, we treated neurons with the transcriptional inhibitor actinomycin for 4 h before inhibiting mTORC1 activity with rapamycin and determined the mRNA levels of CaMKIIα. We predicted that if mTORC1 activity regulates the transcription of CaMKIIα, pretreatment with actinomycin will reflect the same changes in mRNA levels as observed with rapamycin treatment alone. However, if inhibition of mTORC1 kinase activity by rapamycin promotes the degradation of CaMKIIα mRNA, rapamycin treatment in the presence of a transcriptional inhibitor will further decrease the amount of CaMKIIα mRNA. As shown in Fig. 7 D, qPCR analysis of CaMKIIα mRNA levels showed a reduction by 61% (actinomycin, 100 ± 0.9%; actinomycin + rapamycin, 39 ± 18.3%) in neurons treated with both actinomycin and rapamycin relative to actinomycin alone, supporting CaMKIIα mRNA degradation over altered transcription upon mTORC1 inhibition (Fig. 7 D).

Overexpression of CaMKIIα UTRs prevents the increase in dendritic Kv1.1 protein when mTORC1 kinase is inhibited

If HuD binding to Kv1.1 mRNA requires the degradation of high affinity targets such as CaMKIIα mRNA, overexpression of CaMKIIα mRNA containing several HuD binding sites may affect the dendritic expression of Kv1.1 protein. We tested this prediction by overexpressing GFP-fused UTRs of CaMKIIα (5′UTR-GFP-3′UTR of CaMKIIα; Aakalu et al., 2001) in neurons and measured the resulting dendritic Kv1.1 protein levels. The overexpressed CaMKIIα 3′UTR is predicted to carry eight overlapping HuD binding sites (Fig. S4 C). The ability of HuD to promote translation of this construct was first tested in HEK293T cells. Coexpression of HuD and GFP-CaMKIIα UTRs demonstrated a functional interaction by increasing the expression of GFP by approximately threefold over GFP-CaMKIIα UTRs alone (Fig. S4 D, vector-only control [1.00 ± 0.26] and HuD [3.24 ± 0.59]). We then tested whether providing excess CaMKIIα UTRs for HuD binding in neurons will prevent the observed increase in Kv1.1 protein with mTORC1 kinase inhibition. Indeed, dendritic Kv1.1 protein levels no longer

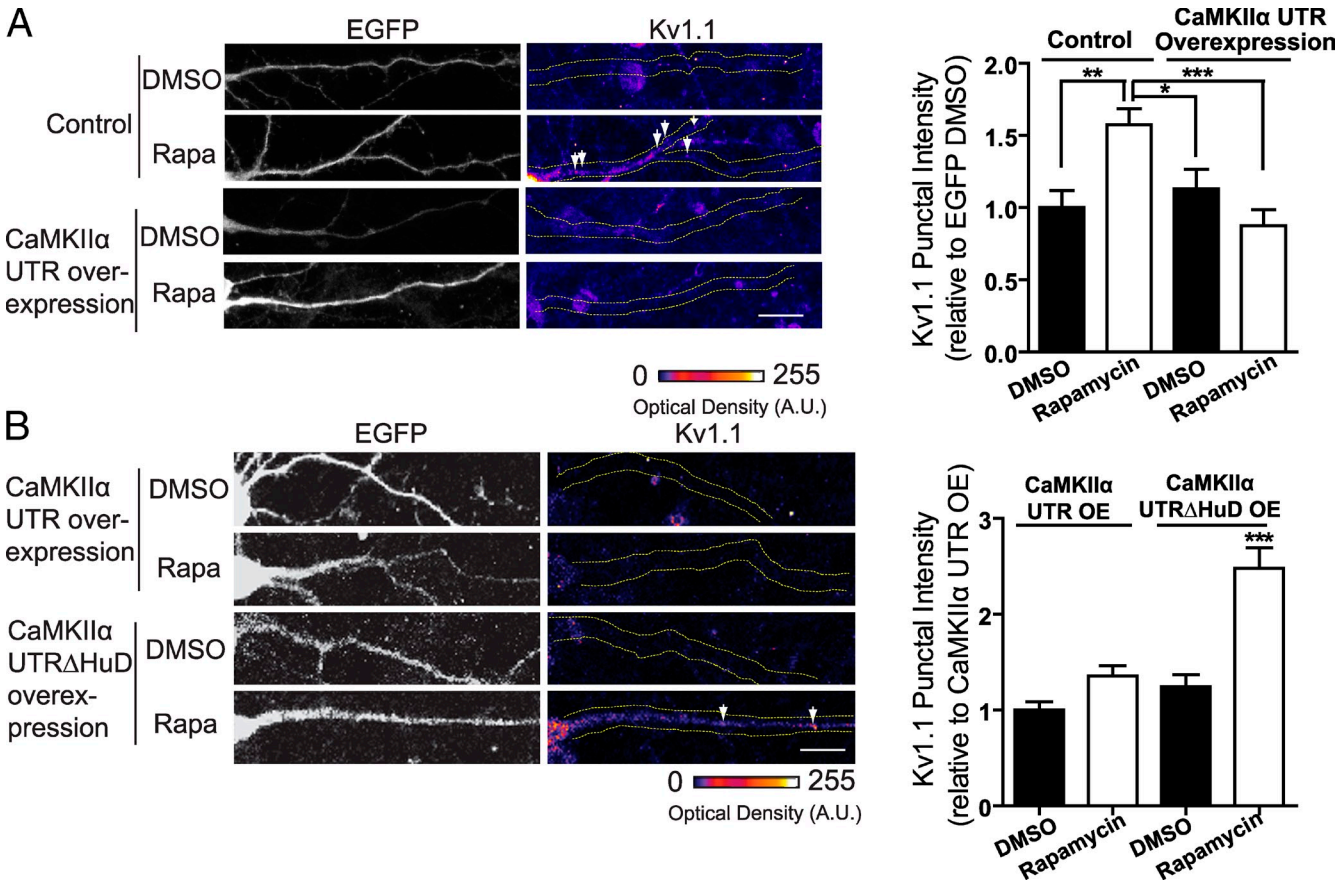

Figure 8. **Overexpression of the CaMKIIα UTR with multiple HuD sites occludes the increase in dendritic Kv1.1 expression.** (A) Representative neurons (DIV 21) transfected with cDNA coding for EGFP or dGFP CaMKIIα UTRs were treated with 200 nM DMSO or rapamycin (Rapa), fixed, and immunostained for EGFP and Kv1.1. Quantification of dendritic Kv1.1 signal intensity for control (EGFP) or CaMKIIα UTR overexpression normalized by baseline signal for dendritic Kv1.1 under control conditions (EGFP/DMSO). Number of dendrites: DMSO-treated control, $n = 22$ and CaMKIIα UTR overexpression (OE), $n = 29$; rapamycin-treated control, $n = 33$ and CaMKIIα UTR overexpression, $n = 31$. *, $P < 0.05$; **, $P < 0.01$; ***, $P < 0.001$; one-way ANOVA, Tukey's posttest. (B) Representative neurons expressing dGFP CaMKIIα UTR without the putative HuD binding sites treated with 200 nM DMSO or rapamycin were quantitated as outlined in A of this figure. Number of dendrites: CaMKIIα UTR overexpression with DMSO control, $n = 20$; CaMKIIα UTR overexpression with rapamycin, $n = 23$; ΔHuD overexpression with DMSO, $n = 20$; ΔHuD overexpression with rapamycin, $n = 24$. ***, $P < 0.001$ relative to all other conditions; one-way ANOVA, Tukey's posttest. Arrows show Kv1.1 puncta (signal). Yellow dotted lines were drawn to outline the representative dendrite. Error bars show SEMs. Bars, 20 µm. A.U., arbitrary unit.

increased with rapamycin treatment in the presence of excess CaMKIIα UTRs (Fig. 8 A, GFP + DMSO [1.00 ± 0.12], GFP + rapamycin [1.58 ± 0.11], CaMKIIα UTRs + DMSO [1.13 ± 0.14], and CaMKIIα UTRs + rapamycin [0.88 ± 0.11]). To verify that repression of Kv1.1 mRNA translation with excess CaMKIIα UTR in the presence of rapamycin is caused by HuD binding this construct, we removed the predicted HuD binding sites within the 3′ UTR (CaMKIIα UTRΔHuD) by PCR-based deletion. Indeed, with mTORC1 inhibition, dendritic Kv1.1 protein expression was restored and insensitive to overexpression of CaMKIIα UTRΔHuD relative to neurons expressing CaMKIIα UTR (Fig. 8 B, CaMKIIα UTRs + DMSO [1.00 ± 0.09], CaMKIIα UTRs + rapamycin [1.36 ± 0.11], CaMKIIα UTRsΔHuD + DMSO [1.24 ± 12], and CaMKIIα UTRsΔHuD + rapamycin [2.48 ± 0.21]). These results suggest that CaMKIIα and Kv1.1 mRNAs compete for HuD binding enabling translation. Collectively, our results support the hypothesis that mTORC1 kinase affects Kv1.1 mRNA translation by changing the availability of HuD via degradation of other high affinity HuD-target mRNAs.

Discussion

Reversible binding of RNA-binding factors to Kv1.1 mRNA with mTORC1 activity regulates dendritic expression of Kv1.1

mTORC1 regulation of Kv1.1 mRNA translation provides an example for how RNA-binding factors may determine the bidirectional expression of dendritic ion channels. As depicted in Fig. S5, our findings support a model in which the levels of Kv1.1 expression can be titrated by the interplay between mTORC1 kinase–dependent reversible binding of miR-129 and HuD to Kv1.1 mRNA. We have provided several lines of evidence demonstrating the repressive role of miR-129. We found that miR-129 binds to Kv1.1 mTRS only when mTORC1 kinase is active and knocking down miR-129 in neurons increases Kv1.1 expression in dendrites, whereas overexpressing miR-129 prevents the rapamycin-dependent increase in dendritic Kv1.1. Consistent with these results, mutating the miR-129 binding site released the local translation of Kv1.1 mRNA from mTORC1 kinase–mediated repression. All these

data suggest that NMDAR activation (Raab-Graham et al., 2006) and mTORC1 kinase signaling may lead to a positive feedback mechanism that reduces the expression of Kv1.1 channels via miR-129, perhaps rendering the dendrite more excitable (Fig. S5, left dendrite).

A major concern of a positive feedback loop is that if left unchecked, it will lead to neuronal instability and prevent further acquisition of new information (Turrigiano and Nelson, 2000). Our findings support a homeostatic mechanism to possibly reduce dendritic excitability by increasing Kv1.1 mRNA translation via the RNA-binding protein HuD. We found that expression of dendritic Kv1.1 is determined by mTORC1 kinase–dependent availability of HuD for Kv1.1 mRNA in the dendrite. We show that HuD binds to high affinity mRNA targets, such as CaMKIIα mRNA, when mTORC1 kinase is active. Those mRNAs degrade when mTORC1 kinase is inhibited, thus releasing HuD to bind to the CR of Kv1.1 mRNA and possibly releasing miR-129–containing miRNA-induced silencing complex from the 3′UTR of this mRNA. Furthermore, neurons overexpressing HuD show protein synthesis–dependent increase of Kv1.1 expression. We thus propose that HuD binds to Kv1.1 mRNA when mTORC1 kinase is inhibited and promotes its translation (Fig. S5, right dendrite). Collectively, our results suggest that mTORC1 kinase serves as a molecular switch for bidirectional changes in dendritic expression of Kv1.1.

One surprising and novel finding from our data is that mTORC1 kinase activity affects the degradation of high affinity HuD mRNA targets, such as CaMKIIα, GAP-43, and Homer1a, instead of affecting miR-129 or HuD levels to favor Kv1.1 mRNA binding. In yeast, rapid degradation of some mRNAs, but not all, has been reported with nutrient limitation or TORC1 kinase inhibition by accelerating the deadenylation–decapping pathway (Albig and Decker, 2001). To our knowledge, our study is the first example of mRNA degradation serving as a way to recycle RNA-binding factors and thus promote the translation of other targets. Consistent with a recycling mechanism, overexpression of CaMKIIα UTRs occludes the increase in dendritic Kv1.1 protein in rapamycin-treated neurons. Furthermore, with mTORC1 inhibition, CaMKIIα UTRs with the HuD binding sites removed rescued this reduction of endogenous dendritic Kv1.1. Our results thus suggest that changing the local availability of the regulatory factors may provide a rapid and spatially restricted response, therefore bypassing the need for new transcription or translation of those factors.

miR-129 and HuD may be important regulators of memory and disease mediated by mTORC1 activity

The importance of miRNAs in neuronal development and plasticity is emerging (Kosik, 2006; Schratt, 2009). miR-129 has been identified to be specifically enriched in the brain (Kim et al., 2004; Miska et al., 2004; Landgraf et al., 2007); however, its role in neuronal function has not been identified. Our data reveal that miR-129 represses the expression of Kv1.1 when mTORC1 is active, which may partially contribute to the increased risk for seizures in disease states with hyperactive mTORC1 kinase (Zeng et al., 2009; Sharma et al., 2010; Sahin, 2012).

The discovery of mTORC1-mediated switching of HuD binding targets provides clues for the importance of mTORC1 in memory. As memory requires both the induction of positive regulators (such as CaMKIIα, which can enhance synaptic strength) and the removal of negative constraints (such as potassium channels that can dampen action potentials; Abel et al., 1998), translational control of those regulators by HuD via mTORC1-mediated mRNA degradation is thus conceivably important for memory. Our findings may thus explain why HuD has been found to be important for memory (Bolognani et al., 2004; Pascale et al., 2004), but overproduction of HuD in transgenic mice led to memory deficits (Bolognani et al., 2007). In other words, the physiological role of HuD may be determined by the ratio of available high to low affinity targets such as CaMKIIα and Kv1.1, respectively.

Because hundreds of dendritic mRNAs have been identified (Martin and Zukin, 2006; Cajigas et al., 2012) and Kv1.1 was the first example of a voltage-gated ion channel being locally translated (Raab-Graham et al., 2006), other mRNAs that are critical to site-specific changes in dendritic excitability may use the same mechanism to regulate their local translation. Our study may thus lead to the future discovery of other functionally related mRNAs suppressed by mTORC1 kinase activity. Moreover, Kv1.1, miR-129, and HuD may serve as important targets and/or biomarkers for mTORC1 kinase–related diseases, such as epilepsy, Fragile X syndrome, tuberous sclerosis complex, and Alzheimer's disease (Richter and Klann, 2009; Sharma et al., 2010).

Materials and methods

Antibodies used

Primary antibodies used were as follows: mouse anti-NeuN (1:500; EMD Millipore), mouse anti-Kv1.1 extracellular, (1:1,000; 75–105; NeuroMab), mouse anti-Kv1.1 (1:1,000; 75–007; NeuroMab), mouse anti-Kv4.2 (75–016; NeuroMab), rabbit anti-Kaede (1:500; PM012; MBL International), rabbit antiphospho-mTOR (1:500; 2971S; Cell Signaling Technology), mouse antitubulin (1:1,000; T6074; Sigma-Aldrich); rabbit anti-HuD (epitope: 26–42 nt; 1:1,000; AB5971; EMD Millipore), rabbit anti-ERK2 (1:1,000; 9108S; Cell Signaling Technology), rabbit antimyc (1:150; c3956; Sigma-Aldrich), rabbit anti-GFP (1:1,000; ab6556; Abcam), and rabbit anti-HuD (for GST pull-down; sc-25360; Santa Cruz Biotechnology, Inc.). Western blot signals were detected by secondary antibodies conjugated to HRP (1:1,000; Jackson ImmunoResearch Laboratories, Inc.) for chemiluminescence or infrared-conjugated secondary antibodies (IR680 at 1:5,000; IR800 at 1:5,000) for the infrared imaging system (Odyssey; LI-COR Biosciences). For immunostaining, secondary antibodies conjugated to either Alexa Fluor 488 (1:400; Invitrogen), Cy3 (1:500; Jackson ImmunoResearch Laboratories, Inc.), Alexa Fluor 647 (1:200; Invitrogen), or Cy5 (1:200; Jackson ImmunoResearch Laboratories, Inc.) were used.

Preparation of primary cultured neurons

Primary neurons were prepared as previously described (Ma et al., 2002). In brief, cortices from embryonic day 18–19 (E18–19) rats were collected, dissociated, and plated. Neurons were plated at densities of 15 million neurons/100-mm dish for affinity RNA capture experiments, 2 million/35-mm well for Western blotting and qPCR, 400,000 neurons/12-mm coverslip for imaging in Fig. 2, and 200,000 neurons/12-mm coverslip for imaging in Fig. 3.

Isolation of SNs and neuronal lysates

SNs were isolated by a modified method as previously described (Quinlan et al., 1999). In brief, neurons were harvested in buffer B (20 mM Hepes, pH 7.4, 5 mM EDTA, pH 8.0, protease inhibitor cocktail [Complete; Roche], phosphatase inhibitor, and RNase inhibitor SUPERase-In [Ambion]

or RNaseOUT [Invitrogen] at 40 U/ml) and homogenized. After pelleting nuclei and unbroken cells at 80 *g* for 10 min, the supernatant was filtered first through a sterile 100-µm nylon filter followed by a 5-µm filter. SN was pelleted at 14,000 *g* for 20 min. For mRNA quantification, total RNA was isolated using RNeasy columns as outlined by the manufacturer (QIAGEN). For miRNA experiments, total RNA was isolated using TRI reagent (Applied Biosystems). For RNA affinity capture, SN pellet was solubilized with radioimmunoprecipitation assay buffer (150 mM NaCl, 10 mM Tris, pH 7.4, 0.1% SDS, 1% Triton X-100, 1% deoxycholate, and 5 mM EDTA supplemented with protease inhibitor cocktail tablet and RNase inhibitor) at 4°C overnight and centrifuged at 55,000 *g* for 1 h to remove any insoluble aggregates. For neuronal lysates, 21 d in vitro (DIV) cultured cortical neurons were harvested, homogenized, and centrifuged similarly as SNs without further filtrations or centrifugation. The supernatant after removing the postsupernatant 1 pellet was collected and used for RNA affinity capture experiments.

Measure SN purity

Before SN preparation, an aliquot was removed and served as the total lysate. Total and concentrated SN was smeared directly onto glass slides, fixed, permeabilized, and then stained using DAPI (1:1,000) wash in PBS. This was imaged using a 20× objective. This staining method was adapted from Williams et al. (2009).

Sindbis virus generation

All the constructs listed in this section were subcloned into SinRep5 virus vector (Invitrogen), and pseudovirions were produced according to the manufacturer's directions.

Kaede-Kv1.1-mTRS. Kaede-Kv1.1 in the SinRep5 vector was digested with BclI. The region of DNA between nt 153 and 1,477 (NCBI Nucleotide accession no. M26161) was dropped out. The backbone DNA was religated.

Kaede-MAP2-DTS. The 3′UTR of MAP2 between nt 2,418 and 3,096 (NCBI Nucleotide accession no. U30938) was cloned by PCR using specific primers, including a NotI restriction site in the forward primer and an XbaI site in the reverse primer (listed in the Primers used section; Blichenberg et al., 1999). The PCR product was digested with NotI and XbaI and ligated into the corresponding restriction sites within the multiple cloning site after the stop codon of Kaede in the Living Color vector (Takara Bio Inc.). Kaede-MAP2-DTS was subcloned into the SinRep5 vector by a blunt-end ligation.

Kaede-Kv1.1, EGFP-Kv1.1 FL, and ΔmiR-129. Kaede or EGFP fused to FL Kv1.1 CR and mTRS were previously cloned into pCDNA3 as described in Raab-Graham et al. (2006). Mutation of miR-129 binding site (seed match sequence) was then achieved by performing site-directed mutagenesis (QuikChange; Agilent Technologies) using primers 5′-CAAAACCAACCAAACAACGTTTTTGAAAAAAAAAAACCCAAC-3′ and 5′-GTTGGGTTTTTTTTTTCAAAAACGTTGTTTGGTTGGTTTTG-3′ (mutations are indicated as underlined sequences). The resulting constructs were then subcloned into SinRep5 vector for virus production.

Competition assays

For Fig. 2, DIV 21 cortical neurons were infected with Sindbis virus coding for Kaede-MAP2-DTS (control) or Kaede-Kv1.1-mTRS. 18 h after infection, neurons were treated with 200 nM DMSO or rapamycin in Hepes-based artificial cerebral spinal fluid (aCSF) for 75 min at 37°C. After treatment, neurons were fixed with 4% paraformaldehyde for 10 min on ice. Neurons were immunostained and imaged as outlined in the Immunofluorescence and image analysis section. Surface expression was quantitated by blindly choosing Kaede-positive neurons.

For Fig. 8, CaMKIIα 5′ → 3′UTR fused to destabilized GFP (dGFP; dGFP-5′, 3′UTR) cDNA was obtained from Addgene, generously deposited there by M. Sutton (University of Michigan, Ann Arbor, MI) and reported by Aakalu et al. (2001). DIV 17 neurons were transfected with EGFP (control) or dGFP- CaMKIIα-5′, 3′UTR cDNA alone. At DIV 21, transfected neurons were treated with 200 nM DMSO or rapamycin for 100 min at 37°C. After treatment, they were fixed with 4% paraformaldehyde for 20 min at RT. Neurons were immunostained and imaged as outlined under immunofluorescence. Putative HuD binding sites were removed by QuikChange mutagenesis using two complimentary oligos (sense strand, 5′-CACTCACACCACTTCCTTCCACCACTCTCTCCCTCTTCCTGGGTTTGGCTC-3′; antisense strand, 5′-CACTCACACCACTTCCTTCCACCACTCTCTCCCTCTTCCTGGGTTTGGCTC-3′). The PCR protocol used to generate loop out was 95°C for 1 min followed by 20 cycles of 95°C for 30 s, 50°C for 1 min, and 68°C for 22 min. Nucleotides removed are highlighted in yellow in Fig. S4 C.

Immunofluorescence and image analysis

Immunofluorescence was performed as outlined in Raab-Graham et al. (2006). For staining of total protein, neurons were fixed with 4% paraformaldehyde, permeabilized with 0.25% Triton X-100, and incubated with primary antibodies overnight at 4°C. Secondary antibodies conjugated to either Alexa Fluor 488 (1:400; Invitrogen), Cy3 (1:500; Jackson ImmunoResearch Laboratories, Inc.), Alexa Fluor 647 (1:200; Invitrogen), or Cy5 (1:200; Jackson ImmunoResearch Laboratories, Inc.) were used in appropriate combinations. For staining of surface-expressed Kv1.1, fixed but nonpermeabilized neurons were incubated overnight at 4°C with Kv1.1 antibody (1:1,000; NeuroMab) that recognizes the extracellular epitope. Neurons were washed extensively with PBS for ≥1 h to remove all excess antibodies before permeabilization. Z-stack images were acquired using an SP5 (DM6000 CFS; Leica) confocal microscope (63× oil objective lens, NA 1.2) by sequential scanning. The LAS AF software (Leica) was used for imaging acquisition. Dendrites were chosen blindly based on Kaede or EGFP signals that were ≥60 µm in length. Signal intensity of puncta was determined by first tracing dendrites ≤150 µm on maximum projected images using the line scan tool in the LAS AF software package. Background was subtracted by determining the signal in a region close to the dendrite but void of all processes. Signal intensity for Kv1.1 puncta was defined as peaks that exceeded the mean signal intensity in control dendrites plus 1 SD.

Cell body analysis

For analysis of cell bodies, a region of interest encompassing the cell body was drawn using ImageJ (National Institutes of Health). The mean intensity was measured for Kv1.1 and normalized to Kaede (Fig. S1 C), DsRed (Fig. S2 F), or EGFP (Fig. S2 E and Fig. S4 B). All integrated signal intensities were between the range of 0 and 255, to ensure that measurements were taken within the linear range.

RNA affinity capture of miRNAs associating with Kv1.1 mRNA

Kv1.1 FL, CR, or ΔmiR129 was PCR amplified using primers containing a T7 promoter and an extra connecting sequence of 20 nt. The PCR products were then purified and in vitro transcribed with T7 polymerase (Ambion) to generate RNA. The RNA fragments were then purified and hybridized with the synthesized biotin oligo (Integrated DNA Technologies) against the 20-nt tag, resulting in 5′-specific biotin labeling of the RNA. 40 µg cell extract from SNs or total neurons was then used to incubate with 4 µg biotinylated RNA for 1 h at RT in reaction buffer (10 mM Hepes, pH 7.4, 150 mM NaCl, 3 mM $MgCl_2$, 2.5% glycerol, 0.5% NP-40, 0.2 mg/ml yeast tRNA, protease inhibitor cocktail, 5 mM EDTA, 40 U/ml RNase inhibitor, and 0.2 mM tris (2-carboxyethyl) phosphine [TCEP]). The associated protein–RNA complex was pulled down with 10 µl streptavidin-coated magnetic beads (Promega) by additional incubation of 1 h at RT. The magnetic beads were then washed three times with reaction buffer and eluted with high salt buffer followed by heating at 95°C for 5 min. The eluent was subjected to miRNA detection using miRNA PCR system (Exiqon) with primers specific for miR-129 (Exiqon).

qPCR for mRNA or miRNA

qPCR was performed by using a SYBR Green PCR Master Mix as outlined by the manufacturer (Applied Biosystems) using a real-time PCR detection system (iCycler IQ; Bio-Rad Laboratories). Fold changes were calculated as outlined by Raab-Graham et al. (2006). For steady-state mRNA quantification (Fig. 1 B), primers against GAPDH were used as an internal housekeeping gene to control for variation between samples. For miRNA pull-down (Fig. 3), 10% total input RNA was used for internal control. All experiments were performed in triplicate. Relative ratios were calculated by the equation, ratio = $(2^{\Delta CPtarget(control\ -\ sample)}/2^{\Delta CPreference(control\ -\ sample)})$, adapted from Pfaffl (2001), in which CP is the threshold cycle, the target is the transcript of interest, and the reference is GAPDH, 5S ribosomal RNA, or 10% total RNA.

Primers used

For cloning of MAP2-DTS, forward primer, 5′-GGCGCGGCCGCGATCTAGCACTAAAATATCATTTTTC-3′, and reverse primer, 5′-GCGGTCTAGATTACTGGACCTTCTTCTTTAGTTACC-3′ were used. For in vitro transcription of RNA for RNA affinity capture assay, Kv1.1 FL forward primer, 5′-CCAAGCTTCTAATACGACTCACTATAGGGAGAGGCCGGACAACGTCAAGGCTATGACGG-3′, and reverse primer, 5′-GTTGGGTTTTTTTTTTCTTTTTGCTTGTTTGG-3′, were used; for mTRS, we used the same forward primer as FL and reverse primer, 5′-TTAAACATCGGTCAGGAGC-3′. For 5′-specific biotinylation of mRNAs, biotin-labeled 5′-AGCCTTGACGTTGTCCGGCC-3′ was used to hybridize with in vitro transcribed mRNAs.

For detection of Kv1.1 mRNA pulled downed by HuD, we used Kv1.1 FL and ΔmiR-129 forward primer, 5′-GCCGCCGCAGCTCCTCTACTATCAG-3′, and reverse primer, 5′-GCTTTTGATTGCTTGCCTGGTGCTT-3′; Kv1.1 CR forward primer, 5′-GGCCATCCTCAGGGTCATCCGCTTG-3′, and reverse primer, 5′-ACACCACCGCCCACCAGAAAGCATC-3′; CaMKIIα forward primer, 5′-CCCTTGGATGTTGCTGGAATTCTC-3′, and reverse primer, 5′-GGGTGGGTCAACACTGGAGACAAAC-3′; GAP-43 forward primer, 5′-GGAATAAGGATCCGAGGAGGAAAGG-3′, and reverse primer, 5′-CTTAAAGTTCAGGCATGTTCTTGGT-3′; GAPDH forward primer, 5′-GCAAGAGAGAGGCCCTCAG-3′, and reverse primer, 5′-TGTGAGGGAGATGCTCAGTG-3′; and Homer1a forward primer, 5′-TGGGTGTCTGGAGTTCTTCCCTTT-3′, and reverse primer, 5′-ATGAAGACCCATCTGCCACGATCA-3′ (adapted from Tiruchinapalli et al., 2008).

LNA transfection of cultured neurons

DIV12 neurons were transfected using Lipofectamine 2000. For each well, 0.4 µg EGFP DNA and 100 nM LNA (either the scrambled or miR-129–specific probes obtained from Exiqon) were used for transfection in a 1:5 dilution with Neurobasal medium. Neurons were incubated with the transfection mix for 2 h at 37°C and returned to conditioned media afterward. 24 h after transfection, neurons were fixed, permeabilized, and immunostained with Kv1.1 antibody as described in the Immunofluorescence and image analysis section. Signal quantitated by blindly choosing EGFP-positive neurons. Fluorescent images of EGFP-transfected neurons and Kv1.1 signals were then taken as outlined in the Immunofluorescence and image analysis section.

miR-129 overexpression assay

Cultured hippocampal neurons were transduced with control or miR-129-2 precursor lentivirus (3×10^5 IU; Biosettia) at DIV 14. Neurons were treated at DIV 21 for 75 min with DMSO or rapamycin. miR-129–overexpressing neurons were detected by immunostaining for DsRed. Kv1.1 surface protein was detected by using an antibody that detects an extracellular domain of Kv1.1 (NeuroMab) using nonpermeabilized neurons.

Northern blot analysis

4 µg of total RNA from DMSO- or rapamycin-treated cells or 2.5 µg of total RNA from scrambled or LNA-transfected cells was separated on a Tris-borate-EDTA-urea-15% polyacrylamide gel. The gel was transferred onto a piece of membrane (Hybond N+; GE Healthcare). The blot was UV cross-linked using a cross-linking system (HL-200 HybriLinker; UVP). The blot was probed for hsa-miR-129-5p miRNA as previously described (Grundhoff et al., 2006). The blot was stripped with boiling hot stripping buffer (0.1% sodium dodecyl sulfate [Sigma-Aldrich] in double-distilled water) and then probed for hsa-let-7a. The sequences for the probes used were as follows: hsa-miR-129-5p, 5′-GCAAGCCCAGACCGCAAAAAG-3′; and hsa-let-7a-5p, 5′-AACTATACAACCTACTACCTCA-3′. Quantitative values for the Northern blot analysis were obtained using the Quantity One Analysis Software (Bio-Rad Laboratories; Grundhoff et al., 2006).

Local translation assay

Local translation assay was performed essentially as reported by Raab-Graham et al. (2006) with the following modifications: primary culture of neurons (DIV 14–28) infected with Sindbis virus coding for Kaede-Kv1.1 FL or Kaede-Kv1.1 ΔmiR-129 for 18–24 h were placed in a 35-mm dish containing Hepes-based aCSF with either 200 nM DMSO or rapamycin and immediately imaged (before photoconversion). Confocal excitation imaging was accomplished using an upright microscope (SP5) with a water immersion lens (HCX Apochromat L20×/0.05 NA water UV to infrared) at RT. A 488-nm laser was used to excite Kaede-Kv1.1, and green emission was detected at 498–534 nm. Serial 1.0-µm z sections of a neuron expressing Kaede-Kv1.1 were acquired and then photoconverted using a DAPI filter for 30 s. After the initial photoconversion, the final image was acquired at 120 min after photoconversion. Maximum projected images from z-compressed stacks were used for data analysis using SP5 software. For each neuron, the mean intensity of 8–10 puncta >60 µm from the soma was measured. All images were analyzed blindly using photoconverted protein as an unbiased selection of puncta. The magnitude of new protein synthesis was calculated by determining the fold increase of the mean green pixel intensity of puncta 120 min after photoconversion (F) as compared with that immediately after photoconversion (F_0; time point 0) and calculated using the equation $\Delta F/F = (F - F_0)/F_0$. Mean basal translation under control conditions (Kaede-Kv1.1 FL with DMSO) was set equal to 100%, and relative new translations measured with rapamycin or Kaede-Kv1.1 ΔmiR-129 ± rapamycin are reported as a percent increase over the mean basal translation.

In situ hybridization of Kv1.1 mRNA in cultured neurons

For in situ hybridization of infected neurons, cultures (DIV 21–28) were infected with Sindbis virus encoding either EGFP-Kv1.1 or EGFP as outlined previously (Raab-Graham et al., 2006). In brief, 18 h after infection, DIV 21–28 neurons were fixed in 4% paraformaldehyde and 4% sucrose for 18 min on ice. Neurons were washed three times in PBS and once in SSC for 5 min. Neurons were permeabilized with 1% Triton X-100 and SSC for 30 min at RT followed by EGFP antisense (nucleotide, 5′-ATATAGACGTTGTGGCTGTTGTAGTTGTACTCCAGCTTCT-3′) digoxigenin-labeled oligo hybridization with an overnight incubation at 37°C. Digoxigenin-labeled oligo was detected using a mouse antidigoxigenin antibody (Roche) followed by an anti–mouse Cy5 antibody (Jackson ImmunoResearch Laboratories, Inc.; laboratory of R.H. Singer, Albert Einstein College of Medicine, New York, NY).

Transfection and isolation of HEK293T cells

HEK293T cells were transfected with Lipofectamine 2000 as outlined by the manufacturer (Invitrogen). 48 h after transfection, cells were harvested by scraping the cells into buffer A (mM: 150 NaCl, 10 Hepes, pH 7.4, 3 KCl, 2 $CaCl_2$, 1 $MgCl_2$, 10 glucose, 250 sucrose, and 5 TCEP) containing protease inhibitors (Complete) and phosphatase inhibitors (Sigma-Aldrich). Cells were lysed by homogenization. Lysates were centrifuged at 106 *g* for 10 min at 4°C. Supernatant was transferred to a new tube and centrifuged for 17,000 *g* for 20 min at 4°C. P2 pellet was resuspended in 100 µl buffer A. SDS sample buffer was added to a final concentration of 1×, and samples were resolved on a 10% SDS-PAGE gel and transferred to nitrocellulose for Western blot analysis.

HuD pull-down of Kv1.1 mRNA from HEK293T cells

HEK293T cells were cotransfected with pCDNA3-myc-HuD and pCDNA3-Kaede-Kv1.1 FL, CR, or ΔmiR-129. pCDNA3 alone and Kaede alone were used as controls. Cell lysates were harvested in polysome lysis buffer (100 mM KCl, 5 mM $MgCl_2$, 10 mM Hepes, 0.5% NP-40, 0.4 µl/ml TCEP, 100 U/ml RNaseOUT, 0.2% vanadyl ribonucleoside complexes, and EDTA-free protease inhibitor tablet) followed by homogenization. After centrifugation at 14,000 *g*, 4°C, for 10 min, the supernatant was precleared with 20 µl/ml protein A/G beads (Santa Cruz Biotechnology, Inc.) for 1 h at 4°C. Protein A/G beads (20 µl/reaction) were coated with myc antibody (2 µg/reaction; Sigma-Aldrich) by incubating at RT for 2 h in NT2 buffer (50 mM Tris, pH 7.4, 150 mM NaCl, 1 mM $MgCl_2$, 0.05% NP-40, 15 mM EDTA, 8 U/ml RNaseOUT, and 0.4 µl/ml TCEP) supplemented with 5% BSA. The myc antibody–coated beads were then washed six times in NT2 buffer. Precleared lysates were incubated with myc antibody–coated beads or beads alone in NT2 buffer supplemented with 3 µl/ml RNaseOUT at 4°C overnight. After washing six times with NT2 buffer, beads were treated with protease K (30 µg/ml in NT2 buffer containing 0.1% SDS) at 55°C for 30 min and subjected to RNA extraction using TRI Reagent LS (Molecular Research Center, Inc.) following the manufacturer's protocol. Purified RNAs were further treated with DNase (TURBO DNase kit; Ambion) following the manufacturer's protocol and used for reverse transcription (SuperScript III kit obtained from Invitrogen) with oligo dT primer. The reverse-transcribed cDNAs were then treated with RNase H (Invitrogen) for 30 min at 37°C and used for PCR with Kv1.1-specific primers (see Primers used section).

HuD overexpression in cultured neurons

Cultured hippocampal neurons were transfected at DIV 12 with cDNAs coding for myc-tagged HuD or pCDNA3 with EGFP. 48 h after transfection, neurons were treated with 50 µM DMSO or cycloheximide for 4 h, fixed, and immunostained with Kv1.1- or Kv4.2-specific antibodies (NeuroMab).

GST pull-down

Neurons were treated at DIV 21 with 200 nM rapamycin or DMSO for 75 min at 37°C in aCSF. Neuronal lysates were isolated in Hepes-based buffer and homogenized. Nuclei and unbroken cells were removed by low speed centrifugation (900 rpm at 10 min), and supernatant was transferred to a new tube containing TRI Reagent LS. RNA was isolated following the manufacturer's instructions (Molecular Research Center, Inc.). 500 ng GST or GST-HuD was incubated with 2.25 µg RNA for 45 min at RT in binding buffer (20 mM Hepes, pH 7.9, 3 mM magnesium acetate, 50 mM potassium acetate, 0.2 µg/µl yeast tRNA, TCEP, RNaseOUT, and 5% glycerol). Protein agarose A/G beads (Santa Cruz Biotechnology, Inc.) were precoated with rabbit pan-Hu antibody in binding buffer or rabbit IgG (Santa Cruz Biotechnology, Inc.) in binding buffer without the yeast tRNA, TCEP, RNaseOUT, and glycerol for 2 h at RT. 50 µl of the precoated IgG beads were used to preclear GST/RNA in solution for 1 h at RT. IgG beads

were removed by centrifugation, and the supernatant was added to pre-coated rabbit anti-HuD beads and incubated for 2 h at RT. Beads were washed with diluted binding buffer (0.5×) without glycerol six times and then eluted with TRI reagent following the manufacturer's protocol (the Direct-zol RNA minikit; Zymo Research). Isolated RNA was treated with DNase I (TURBO DNase kit) and reverse transcribed using the cDNA synthesis kit (iScript; Bio-Rad Laboratories) following the manufacturer's protocol. cDNA was treated with RNase H and subjected to PCR using Kv1.1-, GAP43-, and CaMKIIα-specific primers (see Primers used section). PCR was performed using the SYBR green kit (iQ; Bio-Rad Laboratories). PCR was terminated between cycles 25 and 30 to prevent saturation.

mRNA degradation assay

mRNA degradation assay was performed essentially as previously described (Origanti et al., 2012). In brief, DIV 21 cultured cortical neurons were treated with 12 µM actinomycin for 4 h before the addition of 200 nM rapamycin. Neurons were treated with rapamycin or DMSO plus actinomycin for 75 min in Hepes-based aCSF at 37°C. Neurons were harvested in Hepes-based buffer containing TCEP and RNaseOUT and homogenized. After a low speed centrifugation (900 rpm at 10 min), the supernatant was removed to a new tube containing TRI Reagent LS. RNA was isolated following the manufacturer's instructions (Applied Biosystems). Total RNA was treated with DNase, quantitated, and subjected to RT-qPCR using CaMKIIα-specific primers as outlined under the qPCR for mRNA or miRNA section. Degradation was measured as the percent remaining after treatment with rapamycin as compared with DMSO-treated neurons.

Online supplemental material

Fig. S1, related to Fig. 1 and Fig. 2, shows posttranscriptional regulation of Kv1.1 mRNA mediated by mTRS in the 3′UTR of Kv1.1. Fig. S2 is related to Fig. 3 and displays a schematic representation of the pull-down assay to determine miR-129 binding to Kv1.1, LNA KD of miR-129 in neurons, and cell body analysis of neurons overexpressing miR-129. Fig. S3, related to Fig. 5, includes the quantification of in situ hybridization and EGFP signal between control and neurons expressing Kv1.1 ΔmiR-129. Fig. S4, related to Fig. 6 and Fig. 7, displays the predicted low affinity HuD binding sites present in the CR of Kv1.1 mRNA and that HuD binding to EGFP-CaMKIIα UTR results in increased EGFP levels. Fig. S5 indicates the model supported by the data presented in this paper for the bidirectional regulation of Kv1.1 mRNA translation. Online supplemental material is available at http://www.jcb.org/cgi/content/full/jcb.201212089/DC1.

Thank you to Drs. Robert Messing and Chris Sullivan for their helpful comments.

This work was supported by the National Science Foundation grant IOS-1026527, a University of Texas Research Grant to K.F. Raab-Graham, and by the National Institutes of Health grant 5R01-NS30255 to N.I. Perrone-Bizzozero.

Author contributions: K.F. Raab-Graham, P.P.C. Huang, and N.M. Sosanya conceived and designed the experiments. N.M. Sosanya performed experiments for Fig. 1 B, Fig. 2, Fig. 3 E, Fig. 6 (C and D), Fig. 7 (B–D), Fig. 8 (A and B), and Fig. S1 (A–C). N.M. Sosanya collaborated with L.P. Cacheaux for Fig. 1 A and Fig. 7 A and with P.P.C. Huang for Fig. 3 D and Fig. 6 A. P.P.C. Huang performed experiments for Fig. 3 (A–C) and Fig. S2 (A–E). L.P. Cacheaux performed experiments for Fig. S4 D. C.J. Chen performed Northern blotting experiments. N.I. Perrone-Bizzozero provided Fig. S4 (A and C) and provided HuD cDNAs, GST fusion proteins, and advice. K.F. Raab-Graham performed experiments for Fig. 4, Fig. 5, and Fig. S3 (A and B). K.F. Raab-Graham, P.P.C. Huang, N.I. Perrone-Bizzozero, and N.M. Sosanya wrote the manuscript.

Submitted: 17 December 2012
Accepted: 3 June 2013

References

Aakalu, G., W.B. Smith, N. Nguyen, C. Jiang, and E.M. Schuman. 2001. Dynamic visualization of local protein synthesis in hippocampal neurons. *Neuron*. 30:489–502. http://dx.doi.org/10.1016/S0896-6273(01)00295-1

Abel, T., K.C. Martin, D. Bartsch, and E.R. Kandel. 1998. Memory suppressor genes: inhibitory constraints on the storage of long-term memory. *Science*. 279:338–341. http://dx.doi.org/10.1126/science.279.5349.338

Albig, A.R., and C.J. Decker. 2001. The target of rapamycin signaling pathway regulates mRNA turnover in the yeast *Saccharomyces cerevisiae*. *Mol. Biol. Cell*. 12:3428–3438.

Ando, R., H. Hama, M. Yamamoto-Hino, H. Mizuno, and A. Miyawaki. 2002. An optical marker based on the UV-induced green-to-red photoconversion of a fluorescent protein. *Proc. Natl. Acad. Sci. USA*. 99:12651–12656. http://dx.doi.org/10.1073/pnas.202320599

Antic, D., N. Lu, and J.D. Keene. 1999. ELAV tumor antigen, Hel-N1, increases translation of neurofilament M mRNA and induces formation of neurites in human teratocarcinoma cells. *Genes Dev.* 13:449–461. http://dx.doi.org/10.1101/gad.13.4.449

Bartel, D.P. 2009. MicroRNAs: target recognition and regulatory functions. *Cell*. 136:215–233. http://dx.doi.org/10.1016/j.cell.2009.01.002

Blichenberg, A., B. Schwanke, M. Rehbein, C.C. Garner, D. Richter, and S. Kindler. 1999. Identification of a cis-acting dendritic targeting element in MAP2 mRNAs. *J. Neurosci.* 19:8818–8829.

Bliss, T.V., and T. Lomo. 1973. Long-lasting potentiation of synaptic transmission in the dentate area of the anaesthetized rabbit following stimulation of the perforant path. *J. Physiol.* 232:331–356.

Bolognani, F., and N.I. Perrone-Bizzozero. 2008. RNA-protein interactions and control of mRNA stability in neurons. *J. Neurosci. Res.* 86:481–489. http://dx.doi.org/10.1002/jnr.21473

Bolognani, F., M.A. Merhege, J. Twiss, and N.I. Perrone-Bizzozero. 2004. Dendritic localization of the RNA-binding protein HuD in hippocampal neurons: association with polysomes and upregulation during contextual learning. *Neurosci. Lett.* 371:152–157. http://dx.doi.org/10.1016/j.neulet.2004.08.074

Bolognani, F., D.C. Tanner, M. Merhege, J. Deschênes-Furry, B. Jasmin, and N.I. Perrone-Bizzozero. 2006. In vivo post-transcriptional regulation of GAP-43 mRNA by overexpression of the RNA-binding protein HuD. *J. Neurochem.* 96:790–801. http://dx.doi.org/10.1111/j.1471-4159.2005.03607.x

Bolognani, F., S. Qiu, D.C. Tanner, J. Paik, N.I. Perrone-Bizzozero, and E.J. Weeber. 2007. Associative and spatial learning and memory deficits in transgenic mice overexpressing the RNA-binding protein HuD. *Neurobiol. Learn. Mem.* 87:635–643. http://dx.doi.org/10.1016/j.nlm.2006.11.004

Bolognani, F., T. Contente-Cuomo, and N.I. Perrone-Bizzozero. 2010. Novel recognition motifs and biological functions of the RNA-binding protein HuD revealed by genome-wide identification of its targets. *Nucleic Acids Res.* 38:117–130. http://dx.doi.org/10.1093/nar/gkp863

Brew, H.M., J.L. Hallows, and B.L. Tempel. 2003. Hyperexcitability and reduced low threshold potassium currents in auditory neurons of mice lacking the channel subunit Kv1.1. *J. Physiol.* 548:1–20. http://dx.doi.org/10.1113/jphysiol.2002.035568

Cajigas, I.J., G. Tushev, T.J. Will, S. tom Dieck, N. Fuerst, and E.M. Schuman. 2012. The local transcriptome in the synaptic neuropil revealed by deep sequencing and high-resolution imaging. *Neuron*. 74:453–466. http://dx.doi.org/10.1016/j.neuron.2012.02.036

Chen, X., and D. Johnston. 2010. The elusive D-current: Shaping action potentials in the dendrites? *In* Action Potential: Biophysical and Cellular Context, Initiation, Phases and Propagation. M.L. DuBois, editor. Nova Science Publishers, Inc., Hauppauge, NY. 191–197.

Costa-Mattioli, M., W.S. Sossin, E. Klann, and N. Sonenberg. 2009. Translational control of long-lasting synaptic plasticity and memory. *Neuron*. 61:10–26. http://dx.doi.org/10.1016/j.neuron.2008.10.055

Davis, G.W., and C.S. Goodman. 1998. Genetic analysis of synaptic development and plasticity: homeostatic regulation of synaptic efficacy. *Curr. Opin. Neurobiol.* 8:149–156. http://dx.doi.org/10.1016/S0959-4388(98)80018-4

Deschênes-Furry, J., K. Mousavi, F. Bolognani, R.L. Neve, R.J. Parks, N.I. Perrone-Bizzozero, and B.J. Jasmin. 2007. The RNA-binding protein HuD binds acetylcholinesterase mRNA in neurons and regulates its expression after axotomy. *J. Neurosci.* 27:665–675. http://dx.doi.org/10.1523/JNEUROSCI.4626-06.2007

Fabian, M.R., N. Sonenberg, and W. Filipowicz. 2010. Regulation of mRNA translation and stability by microRNAs. *Annu. Rev. Biochem.* 79:351–379. http://dx.doi.org/10.1146/annurev-biochem-060308-103103

Filipowicz, W., S.N. Bhattacharyya, and N. Sonenberg. 2008. Mechanisms of post-transcriptional regulation by microRNAs: are the answers in sight? *Nat. Rev. Genet.* 9:102–114. http://dx.doi.org/10.1038/nrg2290

Fukao, A., Y. Sasano, H. Imataka, K. Inoue, H. Sakamoto, N. Sonenberg, C. Thoma, and T. Fujiwara. 2009. The ELAV protein HuD stimulates cap-dependent translation in a Poly(A)- and eIF4A-dependent manner. *Mol. Cell*. 36:1007–1017. http://dx.doi.org/10.1016/j.molcel.2009.11.013

Geiger, J.R., and P. Jonas. 2000. Dynamic control of presynaptic Ca(2+) inflow by fast-inactivating K(+) channels in hippocampal mossy fiber boutons. *Neuron*. 28:927–939. http://dx.doi.org/10.1016/S0896-6273(00)00164-1

George, A.D., and S.A. Tenenbaum. 2006. MicroRNA modulation of RNA-binding protein regulatory elements. *RNA Biol.* 3:57–59. http://dx.doi.org/10.4161/rna.3.2.3250

Golding, N.L., H.Y. Jung, T. Mickus, and N. Spruston. 1999. Dendritic calcium spike initiation and repolarization are controlled by distinct potassium channel subtypes in CA1 pyramidal neurons. *J. Neurosci.* 19:8789–8798.

Grimson, A., K.K. Farh, W.K. Johnston, P. Garrett-Engele, L.P. Lim, and D.P. Bartel. 2007. MicroRNA targeting specificity in mammals: determinants beyond seed pairing. *Mol. Cell*. 27:91–105. http://dx.doi.org/10.1016/j.molcel.2007.06.017

Grundhoff, A., C.S. Sullivan, and D. Ganem. 2006. A combined computational and microarray-based approach identifies novel microRNAs encoded by human gamma-herpesviruses. *RNA*. 12:733–750. http://dx.doi.org/10.1261/rna.2326106

Hoeffer, C.A., and E. Klann. 2010. mTOR signaling: at the crossroads of plasticity, memory and disease. *Trends Neurosci.* 33:67–75. http://dx.doi.org/10.1016/j.tins.2009.11.003

Hopkins, W.F., M.L. Allen, K.M. Houamed, and B.L. Tempel. 1994. Properties of voltage-gated K+ currents expressed in *Xenopus* oocytes by mKv1.1, mKv1.2 and their heteromultimers as revealed by mutagenesis of the dendrotoxin-binding site in mKv1.1. *Pflugers Arch.* 428:382–390. http://dx.doi.org/10.1007/BF00724522

Kim, J., and D.A. Hoffman. 2008. Potassium channels: newly found players in synaptic plasticity. *Neuroscientist*. 14:276–286. http://dx.doi.org/10.1177/1073858408315041

Kim, J., A. Krichevsky, Y. Grad, G.D. Hayes, K.S. Kosik, G.M. Church, and G. Ruvkun. 2004. Identification of many microRNAs that copurify with polyribosomes in mammalian neurons. *Proc. Natl. Acad. Sci. USA*. 101:360–365. http://dx.doi.org/10.1073/pnas.2333854100

Klann, E., and T.E. Dever. 2004. Biochemical mechanisms for translational regulation in synaptic plasticity. *Nat. Rev. Neurosci.* 5:931–942. http://dx.doi.org/10.1038/nrn1557

Konecna, A., J.E. Heraud, L. Schoderboeck, A.A. Raposo, and M.A. Kiebler. 2009. What are the roles of microRNAs at the mammalian synapse? *Neurosci. Lett.* 466:63–68. http://dx.doi.org/10.1016/j.neulet.2009.06.050

Kosik, K.S. 2006. The neuronal microRNA system. *Nat. Rev. Neurosci.* 7:911–920. http://dx.doi.org/10.1038/nrn2037

Kundu, P., M.R. Fabian, N. Sonenberg, S.N. Bhattacharyya, and W. Filipowicz. 2012. HuR protein attenuates miRNA-mediated repression by promoting miRISC dissociation from the target RNA. *Nucleic Acids Res.* 40:5088–5100. http://dx.doi.org/10.1093/nar/gks148

Kuwano, Y., H.H. Kim, K. Abdelmohsen, R. Pullmann Jr., J.L. Martindale, X. Yang, and M. Gorospe. 2008. MKP-1 mRNA stabilization and translational control by RNA-binding proteins HuR and NF90. *Mol. Cell. Biol.* 28:4562–4575. http://dx.doi.org/10.1128/MCB.00165-08

Landgraf, P., M. Rusu, R. Sheridan, A. Sewer, N. Iovino, A. Aravin, S. Pfeffer, A. Rice, A.O. Kamphorst, M. Landthaler, et al. 2007. A mammalian microRNA expression atlas based on small RNA library sequencing. *Cell*. 129:1401–1414. http://dx.doi.org/10.1016/j.cell.2007.04.040

Ma, D., N. Zerangue, K. Raab-Graham, S.R. Fried, Y.N. Jan, and L.Y. Jan. 2002. Diverse trafficking patterns due to multiple traffic motifs in G protein-activated inwardly rectifying potassium channels from brain and heart. *Neuron*. 33:715–729. http://dx.doi.org/10.1016/S0896-6273(02)00614-1

Martin, K.C., and R.S. Zukin. 2006. RNA trafficking and local protein synthesis in dendrites: an overview. *J. Neurosci.* 26:7131–7134. http://dx.doi.org/10.1523/JNEUROSCI.1801-06.2006

Meisner, N.C., and W. Filipowicz. 2011. Properties of the regulatory RNA-binding protein HuR and its role in controlling miRNA repression. *Adv. Exp. Med. Biol.* 700:106–123. http://dx.doi.org/10.1007/978-1-4419-7823-3_10

Metz, A.E., N. Spruston, and M. Martina. 2007. Dendritic D-type potassium currents inhibit the spike afterdepolarization in rat hippocampal CA1 pyramidal neurons. *J. Physiol.* 581:175–187. http://dx.doi.org/10.1113/jphysiol.2006.127068

Miska, E.A., E. Alvarez-Saavedra, M. Townsend, A. Yoshii, N. Sestan, P. Rakic, M. Constantine-Paton, and H.R. Horvitz. 2004. Microarray analysis of microRNA expression in the developing mammalian brain. *Genome Biol.* 5:R68. http://dx.doi.org/10.1186/gb-2004-5-9-r68

Monaghan, M.M., J.S. Trimmer, and K.J. Rhodes. 2001. Experimental localization of Kv1 family voltage-gated K+ channel alpha and beta subunits in rat hippocampal formation. *J. Neurosci.* 21:5973–5983.

Origanti, S., S.L. Nowotarski, T.D. Carr, S. Sass-Kuhn, L. Xiao, J.Y. Wang, and L.M. Shantz. 2012. Ornithine decarboxylase mRNA is stabilized in an mTORC1-dependent manner in Ras-transformed cells. *Biochem. J.* 442:199–207. http://dx.doi.org/10.1042/BJ20111464

Pascale, A., P.A. Gusev, M. Amadio, T. Dottorini, S. Govoni, D.L. Alkon, and A. Quattrone. 2004. Increase of the RNA-binding protein HuD and posttranscriptional up-regulation of the GAP-43 gene during spatial memory. *Proc. Natl. Acad. Sci. USA*. 101:1217–1222. http://dx.doi.org/10.1073/pnas.0307674100

Pfaffl, M.W. 2001. A new mathematical model for relative quantification in real-time RT-PCR. *Nucleic Acids Res.* 29:e45. http://dx.doi.org/10.1093/nar/29.9.e45

Quinlan, E.M., B.D. Philpot, R.L. Huganir, and M.F. Bear. 1999. Rapid, experience-dependent expression of synaptic NMDA receptors in visual cortex in vivo. *Nat. Neurosci.* 2:352–357. http://dx.doi.org/10.1038/7263

Raab-Graham, K.F., P.C. Haddick, Y.N. Jan, and L.Y. Jan. 2006. Activity- and mTOR-dependent suppression of Kv1.1 channel mRNA translation in dendrites. *Science*. 314:144–148. http://dx.doi.org/10.1126/science.1131693

Richter, J.D., and E. Klann. 2009. Making synaptic plasticity and memory last: mechanisms of translational regulation. *Genes Dev.* 23:1–11. http://dx.doi.org/10.1101/gad.1735809

Ronesi, J.A., and K.M. Huber. 2008. Homer interactions are necessary for metabotropic glutamate receptor-induced long-term depression and translational activation. *J. Neurosci.* 28:543–547. http://dx.doi.org/10.1523/JNEUROSCI.5019-07.2008

Sahin, M. 2012. Targeted treatment trials for tuberous sclerosis and autism: no longer a dream. *Curr. Opin. Neurobiol.* 22:895–901. http://dx.doi.org/10.1016/j.conb.2012.04.008

Schechter, L.E. 1997. The potassium channel blockers 4-aminopyridine and tetraethylammonium increase the spontaneous basal release of [3H]5-hydroxytryptamine in rat hippocampal slices. *J. Pharmacol. Exp. Ther.* 282:262–270.

Schratt, G. 2009. Fine-tuning neural gene expression with microRNAs. *Curr. Opin. Neurobiol.* 19:213–219. http://dx.doi.org/10.1016/j.conb.2009.05.015

Sharma, A., C.A. Hoeffer, Y. Takayasu, T. Miyawaki, S.M. McBride, E. Klann, and R.S. Zukin. 2010. Dysregulation of mTOR signaling in fragile X syndrome. *J. Neurosci.* 30:694–702. http://dx.doi.org/10.1523/JNEUROSCI.3696-09.2010

Smart, S.L., V. Lopantsev, C.L. Zhang, C.A. Robbins, H. Wang, S.Y. Chiu, P.A. Schwartzkroin, A. Messing, and B.L. Tempel. 1998. Deletion of the K(V)1.1 potassium channel causes epilepsy in mice. *Neuron*. 20:809–819. http://dx.doi.org/10.1016/S0896-6273(00)81018-1

Southan, A.P., and D.G. Owen. 1997. The contrasting effects of dendrotoxins and other potassium channel blockers in the CA1 and dentate gyrus regions of rat hippocampal slices. *Br. J. Pharmacol.* 122:335–343. http://dx.doi.org/10.1038/sj.bjp.0701392

Srikantan, S., K. Tominaga, and M. Gorospe. 2012. Functional interplay between RNA-binding protein HuR and microRNAs. *Curr. Protein Pept. Sci.* 13:372–379. http://dx.doi.org/10.2174/138920312801619394

Storm, J.F. 1988. Temporal integration by a slowly inactivating K+ current in hippocampal neurons. *Nature*. 336:379–381. http://dx.doi.org/10.1038/336379a0

Tanouye, M.A., and A. Ferrus. 1985. Action potentials in normal and Shaker mutant *Drosophila*. *J. Neurogenet.* 2:253–271. http://dx.doi.org/10.3109/01677068509102322

Tiffany, A.M., L.N. Manganas, E. Kim, Y.P. Hsueh, M. Sheng, and J.S. Trimmer. 2000. PSD-95 and SAP97 exhibit distinct mechanisms for regulating K^+ channel surface expression and clustering. *J. Cell Biol.* 148:147–158. http://dx.doi.org/10.1083/jcb.148.1.147

Tiruchinapalli, D.M., M.D. Ehlers, and J.D. Keene. 2008. Activity-dependent expression of RNA binding protein HuD and its association with mRNAs in neurons. *RNA Biol.* 5:157–168. http://dx.doi.org/10.4161/rna.5.3.6782

Turrigiano, G.G., and S.B. Nelson. 2000. Hebb and homeostasis in neuronal plasticity. *Curr. Opin. Neurobiol.* 10:358–364. http://dx.doi.org/10.1016/S0959-4388(00)00091-X

Vatolin, S., K. Navaratne, and R.J. Weil. 2006. A novel method to detect functional microRNA targets. *J. Mol. Biol.* 358:983–996. http://dx.doi.org/10.1016/j.jmb.2006.02.063

Volk, L.J., B.E. Pfeiffer, J.R. Gibson, and K.M. Huber. 2007. Multiple Gq-coupled receptors converge on a common protein synthesis-dependent long-term depression that is affected in fragile X syndrome mental retardation. *J. Neurosci.* 27:11624–11634. http://dx.doi.org/10.1523/JNEUROSCI.2266-07.2007

Wang, X., and T.M. Tanaka Hall. 2001. Structural basis for recognition of AU-rich element RNA by the HuD protein. *Nat. Struct. Biol.* 8:141–145. http://dx.doi.org/10.1038/84131

Wells, D.G., X. Dong, E.M. Quinlan, Y.S. Huang, M.F. Bear, J.D. Richter, and J.R. Fallon. 2001. A role for the cytoplasmic polyadenylation element in NMDA receptor-regulated mRNA translation in neurons. *J. Neurosci.* 21:9541–9548.

Williams, C., R. Mehrian Shai, Y. Wu, Y.H. Hsu, T. Sitzer, B. Spann, C. McCleary, Y. Mo, and C.A. Miller. 2009. Transcriptome analysis of synaptoneurosomes identifies neuroplasticity genes overexpressed in incipient Alzheimer's disease. *PLoS ONE*. 4:e4936. http://dx.doi.org/10.1371/journal.pone.0004936

Wu, J., J. Qian, C. Li, L. Kwok, F. Cheng, P. Liu, C. Perdomo, D. Kotton, C. Vaziri, C. Anderlind, et al. 2010. miR-129 regulates cell proliferation by

downregulating Cdk6 expression. *Cell Cycle*. 9:1809–1818. http://dx.doi.org/10.4161/cc.9.9.11535

Xue, Y., K. Ouyang, J. Huang, Y. Zhou, H. Ouyang, H. Li, G. Wang, Q. Wu, C. Wei, Y. Bi, et al. 2013. Direct conversion of fibroblasts to neurons by reprogramming PTB-regulated microRNA circuits. *Cell*. 152:82–96. http://dx.doi.org/10.1016/j.cell.2012.11.045

Zeng, L.H., N.R. Rensing, and M. Wong. 2009. The mammalian target of rapamycin signaling pathway mediates epileptogenesis in a model of temporal lobe epilepsy. *J. Neurosci.* 29:6964–6972. http://dx.doi.org/10.1523/JNEUROSCI.0066-09.2009

Zerr, P., J.P. Adelman, and J. Maylie. 1998. Episodic ataxia mutations in Kv1.1 alter potassium channel function by dominant negative effects or haploinsufficiency. *J. Neurosci.* 18:2842–2848.

Zhang, W., and D.J. Linden. 2003. The other side of the engram: experience-driven changes in neuronal intrinsic excitability. *Nat. Rev. Neurosci.* 4:885–900. http://dx.doi.org/10.1038/nrn1248